2014

Statistical analysis of multiple hydrostatic pump flow loss models

Samuel Jason Hall
Iowa State University

`

Statistical analysis of multiple hydrostatic pump flow loss models

by

Samuel Jason Hall

A thesis submitted to the graduate faculty

in partial fulfillment of the requirements for the degree of

MASTER OF SCIENCE

Major: Agricultural and Biosystems Engineering

Program of Study Committee:
Brian L. Steward, Major Professor
Stuart J. Birrell
Greg R. Luecke

Iowa State University

Ames, Iowa

2014

TABLE OF CONTENTS

LIST OF FIGURES

LIST OF TABLES

LIST OF VARIABLES

a	Pressure dependent constant within the laminar leakage coefficient (Dorey model)
a_0	Flow dependent coefficient
a_1	Displacement independent compressibility coefficient (Rydberg model)
a_2	Displacement dependent compressibility coefficient (Rydberg model)
a_3	Laminar flow coefficient (Rydberg model)
a_4	Analytical loss coefficient (best fit for axial piston pumps) (Rydberg model)
A_{piston}	Cross sectional area of a piston
b:	pressure and flow dependent constant within the laminar leakage coefficient (Dorey model)
C_1, C_2, C_3, C_4, C_5	Loss coefficients (Zarotti and Nevegna model)
C_{C1}	Displacement independent compressibility coefficient (Olsson model)
C_{C2}	Displacement dependent compressibility coefficient (Olsson model)
C_{const}	Constant flow loss term
C_{CP}	Viscous flow coefficient (Pacey, Turquist and Clark model)
C_S	Laminar flow loss coefficient
C_S^*	Non-linear laminar flow loss coefficient (Dorey)
C_{ST}	Turbulent flow loss coefficient
C_{VN}	Valve plate notch loss coefficient (Jeong model)
C_{vPV}	Couette flow coefficient (Jeong model)
C_β	Bulk Modulus loss coefficient (Jeong model)
$C_{\mu PSV}$	Laminar flow loss coefficient (Jeong model)
d_{piston}	Diameter of a piston
f_{Pmax}	Displacement dependent polynomial fitted flow loss rate at maximum pressure (Huhtala model)
f_{Pmin}	Displacement dependent polynomial fitted flow loss rate at maximum pressure (Huhtala model)
f_v	Displacement setting dependent flow losses (Huhtala model)
$f_{\mu max}$	Pressure dependent polynomial fitted flow loss rate at maximum Viscosity (Huhtala model)
$f_{\mu min}$	Pressure dependent polynomial fitted flow loss rate at minimum Viscosity (Huhtala model)

H_{stroke}	Stroke height of the rotating group of an axial piston pump
$I_{01} - I_{54}$	Model coefficients with exponents 2,2,2 and 1 (Ivantysyn and Ivantysynova model)
k	Kinematic viscosity constant
k_{ijk}:	Loss coefficient (Ivantysyn and Ivantysynova model)
$K_{Q1} - K_{Q12}$:	Loss Coefficients (Kögl model)
n_{max}	Maximum operating speed of an axial piston pump
n_{min}	Minimum operating speed of an axial piston pump
n_{pump}	Pump input shaft speed
p_{atm}	Atmospheric Pressure
p_{case}	Pressure in the pump case
p_{hp}	Pressure on the pump outlet
p_{lp}	Pressure at the pump inlet
p_{max}	Maximum pressure in the measured data set (Huhtala model)
p_{min}	Minimum pressure in the measured data set (Huhtala model)
Δp_{sys}	Pressure rise from the pump inlet to outlet
$\Delta q_{V2,e}$	Average change in flow (from ISO 8426)
$Q_{B.mod}$	Effective flow due to fluid decompression
$q_1 - q_4$:	Loss Coefficients: (Ortwig)
Q_{ideal}	Flow from pump based on ideal displacement
Q_L	Total Flow Loss
Q_{L_COMP}	Compressibility flow loss coefficient (Bavendiek)
$Q_{L1} - Q_{L8}$	Flow loss coefficients (Bavendiek)
$Q_{L,ext}$	Flow losses that flow into the pump case
$Q_{L,int}$	Flow losses that flow back to the pump inlet
Q_{Lo}	Constant flow loss (Jeong model)
$q_{n,max}$	Pressure dependent polynomial fitted flow loss rate at maximum Pressure (Huhtala model)
Q_{meas}	System flow measured after the relief valve
$q_{n,min}$	Pressure dependent polynomial fitted flow loss rate at minimum Pressure (Huhtala model)
Q_{Pmax}	Speed dependent polynomial fitted flow loss rate at maximum pressure (Huhtala model)
Q_{Pmin}	Speed dependent polynomial fitted flow loss rate at minimum pressure(Huhtala model)
Q_{outlet}	System flow out of the pump
$Q_{v_{n,p}}$	Pressure and speed dependent flow loss (Huhtala model)
R_{piston}	Piston pitch radius in an axial piston pump
T_{oil}	Oil temperature relative to a reference condition

$\boldsymbol{V_{max}}$	Maximum displacement of an axial piston pump
$\boldsymbol{V_p}$	Ideal pump displacement
$\boldsymbol{V_R}$	Ratio between the dead volume of the axial piston rotating group and displacement
$\boldsymbol{z}$	Number of pistons in a pump
$\boldsymbol{\alpha}$	Swash angle of an axial piston pump
$\boldsymbol{\beta_0}$	Reference bulk modulus of the fluid.
β_{fit}	Bulk modulus at fitting point (Huhtala model)
$\boldsymbol{\beta_{oil}}$	Bulk modulus of the fluid
$\boldsymbol{\beta_p}$	Isothermal compressibility coefficient of fluid,
$\boldsymbol{\beta_T}$	Volumetric expansion coefficient of fluid,
$\boldsymbol{\varepsilon_p}$	Coefficient of displacement
$\boldsymbol{\eta_0}$	Reference kinematic viscosity
$\boldsymbol{\mu}$:	Hydraulic fluid viscosity
$\boldsymbol{\mu_{max}}$	Maximum viscosity in the measured data set (Huhtala model)
$\boldsymbol{\mu_{min}}$	Minimum viscosity in the measured data set (Huhtala model)
$\boldsymbol{\rho}$:	Hydraulic fluid density
$\boldsymbol{\rho_0}$	The oil density at a reference condition
$\boldsymbol{\rho_T}$	Rate of change of oil density with temperature

Regression, Multicollinearity and Cross Validation

$\boldsymbol{k}$:	Number of independent coefficients in a linear model
$\hat{\boldsymbol{L}}$:	Maximized value of the likelihood function for a model
$\boldsymbol{n}$:	Number of samples in the regression data set
$\boldsymbol{R}$	Pearson correlation coefficient
$\boldsymbol{R^2}$	Coefficient of determination of a model coefficient
$\boldsymbol{X}$	Independent variable (linear regression)
$\boldsymbol{y}$	Dependent variable (linear regression)
$\hat{\boldsymbol{y}}$	Modeled value of the independent variable
$\boldsymbol{\beta}$	Regression coefficient (linear regression)
$\hat{\boldsymbol{\beta}}$	Estimated regression coefficient (linear regression)
$\boldsymbol{\varepsilon}$	Error (linear regression)

ABSTRACT

Tier 4 legislation and rising fuel prices have increased the attention dedicated to increasing efficiency by designers of off highway vehicles and their components. This paper discusses a methodology for comparing flow loss models of closed circuit axial piston pumps, which are common on off-highway vehicle propulsion systems. Having the best mathematical representation of the flow losses in the pump will aid the designers in understanding the impacts of loss on their vehicle's efficiency. Five flow loss models were compared including the: 1) Wilson, 2) Schlösser, 3) Zarotti and Nevegna 4) Ivantysyn and Ivantysynova and 5) Jeong models. The methodology consists of four steps for the comparison of flow losses: 1) calibration of complete models, 2) parameter reduction through stepwise regression, 3) parameter reduction by reducing multicollinearity and 4) a leave one out cross validation (LOOCV). Of all five, the Ivantysyn and Ivantysynova model clearly calibrated to the measured data set the closest with an root mean squared error of 0.305 L/min. However, in performing cross validation, there does not appear to be a significant difference between the Zarotti and Nevegna, Ivantysyn and Ivantysynova and the Jeong models in their capability to estimate measured flow losses.

CHAPTER 1. GENERAL INTRODUCTION

1.1 Introduction

Legislation in the United States has mandated that the amount of pollution emitted by non-road vehicles (also known as off-highway vehicles) utilizing diesel engines must be reduced significantly. The new pollution controls will reduce the amount of NO_x and particulate material exhausted into the atmosphere [1] within allowable pollutant levels (Fig 1.1). The EPA has estimated the by the year 2030 these reductions will prevent 12,000 premature deaths, save 8,900 hospitalizations and one million lost work days annually [2].

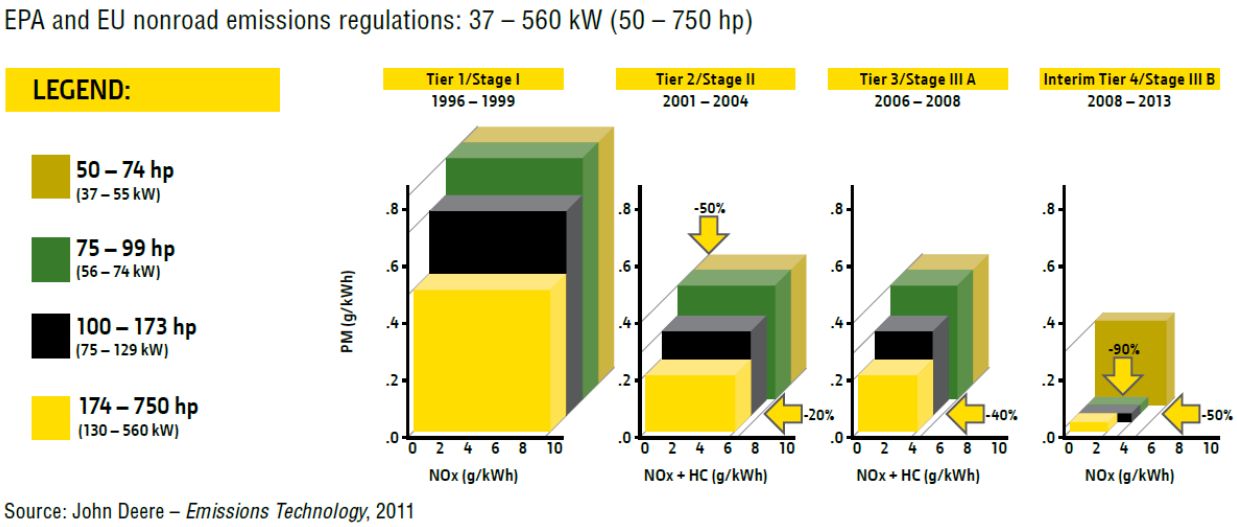

Figure 1.1. Graphic showing the decreases in pollutants required by EPA / EU regulations from Tier 1 to Tier 4i.

To accomplish these reductions engine manufacturers have chosen one of two systems to meet the criteria set by the EPA final rule for Tier IV. First, systems with exhaust gas recirculation (EGR) mixes exhaust gas back in with fresh air into the combustion chamber to reduce combustion temperatures. Secondly, selective catalytic reduction (SCR) systems mix a water/urea mixture into the exhaust gas to

turn the nitrogen oxides from the exhaust into nitrogen gas and water. Both of these methods increase the total cost of ownership to the end user; EGR reduces engine efficiency and SCR adds cost to the engine and requires diesel exhaust fluid for proper function. One large off-road, construction vehicle company is raising prices of all of vehicles by nearly twelve percent due to R&D and after-treatment system costs [3].

For the vehicle manufacturer, efficiency in all of the systems powered by the engine must be increased. Hydraulic systems are being examined not only in industry, but also in academia, as a target system where efficiency gains for off-road machines can be accomplished. All components of a hydraulic system (pumps, motors, valves, etc.) as well as circuit concepts are being studied to reduce energy loss. Fluid power systems on average are estimated to be only 22% energy efficient, with around one third of the inefficiencies directly attributable to component losses [4]. A better understanding of the efficiency of individual components will help designers build more efficient hydraulic systems.

Hydrostatic transmissions (HSTs) are a type of hydraulic system that transmit mechanical power from the engine to a ground drive mechanism (wheel, mechanical drive for a tracked or wheeled vehicle) and to fan drive systems for cooling (Fig 1.2). These systems are called closed circuit systems since only a small portion of the hydraulic flow is returned back to the reservoir with the majority flowing around the circuit. These systems typically include a primary hydraulic pump that flows oil directly to a hydraulic motor; a “charge” pump is also adding flow to the low pressure side of the loop. In addition to the pumps and motors, relief and check valves are

needed to maintain charge pressure on the low-pressure line returning flow from the motor to the pump. The efficiency of the HST components has a direct effect on overall vehicle efficiency [5].

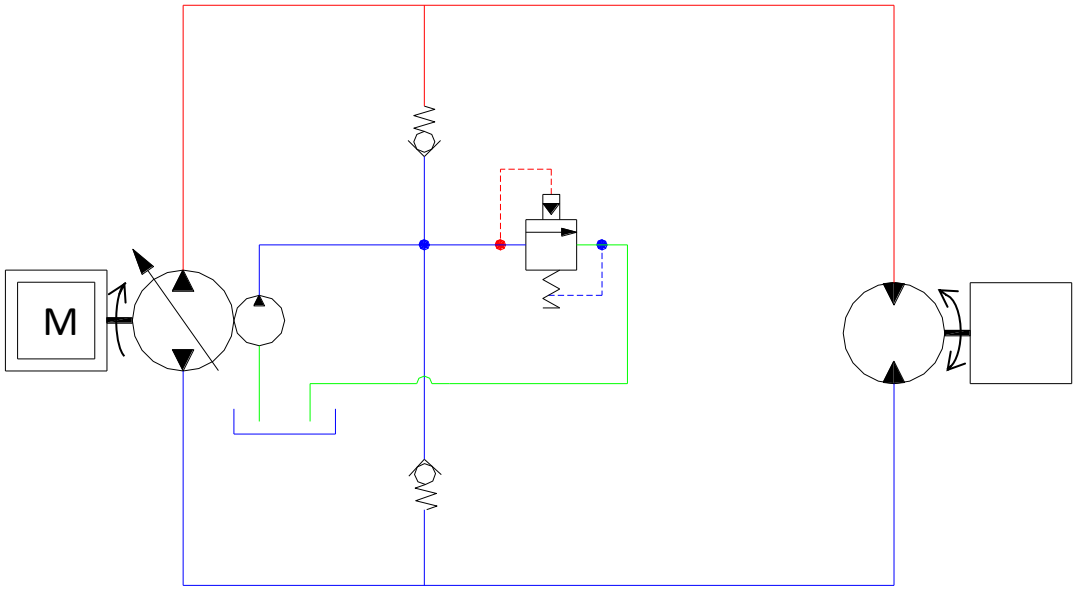

Figure 1.2. Basic schematic of a HST. Included are prime mover, hydrostatic pump, charge pump, charge relief valve, charge check valves, hydrostatic motor and load.

A number of authors have developed mathematical models to characterize both the volumetric and mechanical losses or efficiency of hydraulic pumps and motors. Approaches are generally sorted into three categories [6]: 1) physical, 2) analytical and 3) numerical. Physical models are based singularly on first-principle descriptions of the physical system. Analytical models are not limited to only loss terms based on physical principles and typically include non-linear terms that better explain variability in measured losses. These models include terms that model physical processes as well as terms that aid in fitting data. Numerical loss models characterize loss behavior by approximation. The individual terms of the model generally have little physical meaning and are assembled to fit the data as best as

possible. Numerical models can only be determined by fitting parameters to a large data set.

1.2 Research Objectives

The overarching objective is to develop a clear methodology for comparing flow loss models for axial piston pumps. Within that framework, a group of flow loss models from the literature were compared through the methodology. The first objective is to determine how well each of the models can be calibrated to a common data set. The second objective is to determine if reduced versions of the original models can be developed without loss of performance. The third objective is to ensure that the models are characterizing the pump flow loss and not over characterizing the specific measured data set. At the same time, an indication of how well each of the models will predict flow losses relative to one another will be found. The overall goal of this thesis is to contribute to the knowledge of flow loss modeling in axial piston pumps and draw attention to the statistical issues that may arise from using any of the current or future models.

1.3 Organization of the Thesis

The thesis is organized into four chapters. An introduction to the research context is presented in this thesis chapter (Ch. 1). Chapter two will present an exhaustive literature review of methods used to determine the ideal displacement of hydraulic pumps and steady state flow loss models of hydraulic pumps. Each of these models is discussed in detail. A subset of these methods and models presented will be used in the primary research work of this thesis.

Chapter three presents an article prepared for publication in a peer reviewed journal. It presents a comparison of five flow loss models that are representative examples of those found in the literature review. The models were calibrated, reduced, and cross-validated to a data set acquired during product development at Danfoss Power Solutions in Ames, Iowa. General conclusions derived from the work and recommendations for the future work are presented in Chapter four of the thesis.

REFERENCES

[1] The John Deere Company, 2011, “Emissions Technology – Nonroad Diesel Engines” , retrieved on 2/8/2014, http://pdf.directindustry.com/pdf/john-deere-power-systems/emissions-technology/23111-20657-_4.html.

[2] Federal Register (US), 2004, “Control of Emissions of Air Pollution From Nonroad Diesel Engines and Fuel; Final Rule,” Vol. 69 No. 124, 2004, June 29. Retrieved January 02, 2012, http://www.gpo.gov/fdsys/pkg/FR-2004-06-29/pdf/04-11293.pdf.

[3] Kenny, K., 2010, “Caterpillar Showcases Tier 4 Interim//Stage IIIB Readiness and Leadership”, press release Feb. 11, 2010, retrieved on 2/8/2014, http://indonesia.cat.com/cda/files/2076717/7/021110%20Caterpillar%20Showcases%20Tier%204%20Interim%20Stage%20IIIB%20Readiness%20and%20Leadership.pdf.

[4] Love, L., Lanke, E., Alles, P., 2012, “Estimating the Impact (Energy, Emissions and Economics) of the U.S. Fluid Power Industry,” Oak Ridge National Laboratory – United States Department of Energy, ORNL/TM-2011/14.

[5] Ivantysyn J. and Ivantysynova M., 2000, “Hydrostatic Pumps and Motors, Principals, Designs, Performance, Modeling, Analysis, Control and Testing”, New Delhi: Academia Books International.

[6] Kohmäscher, T., Rahmfeld, R., Murrenhoff, H., Skirde, E., 2007, “Improved loss modelingof hydrostatic units – requirement for precise simulation of mobile working machine drivelines,” 2007 Proceedings of ASME International Mechanical Engineering Congress and Exposition, Paper 41803.

CHAPTER 2. IDEAL DISPLACEMENT AND FLOW LOSS MODELING BACKGROUND

2.1 Introduction

The work in this thesis examines mathematical modeling of flow loss in axial piston pumps. This chapter presents the background information of how both the ideal displacement of a pump can be determined using measured data or displacement element dimensions, and how previous authors have quantified flow losses. One ideal displacement calculation method and five flow loss models were used in the primary work of this thesis.

This thesis concentrates on modeling flow losses of positive displacement, axial piston pumps. It is important to ensure that the terminology used to describe the mathematical representation of the pump has a clear connection to the physical hardware and operating characteristics. The rotating group along with the variable swash plate determines the ideal displacement of the pump (Fig. 2.1). As the input shaft rotates, flow is produced by drawing fluid into the low-pressure inlet and displacing the fluid to the high-pressure side. The volume captured within the housing and the end-cap, but outside the rotating group is referred to as the pump case volume. The pressure of the fluid within the pump case volume appears in many of the loss models throughout this chapter. The valve-plate ports oil between the rotating group and the end-cap to ensure that the flow is as uniform as possible and still maintain the desired efficiency of the pump.

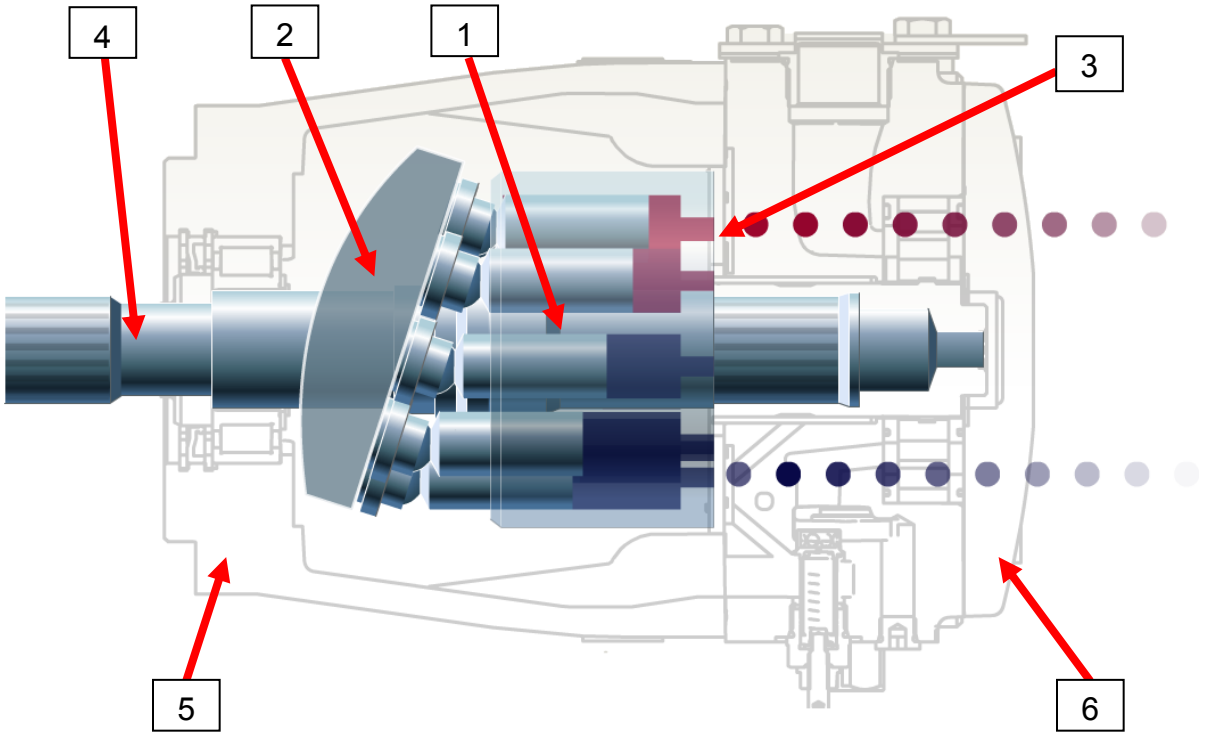

Figure 2.1. Internal components of an axial piston pump. Primary components include: 1) rotating group, 2) swash-plate, 3) valve-plate, 4) input shaft, 5) housing and 6) end-cap. (courtesy Danfoss Power Solutions).

The remainder of this chapter is separated into three primary sections: 1) methods of determining the ideal displacement of the pump and 2) a detailed description of the notable flow loss models and 3) a discussion and comparison of the flow loss models. This review of the literature will provide the background necessary for the characterizing flow losses within an axial piston pump.

2.2 Ideal Displacement

The ideal displacement of an axial piston pump is defined as the volume that is swept by the rotating group per revolution of the input shaft. The pump would have zero flow loss if the measured flow out of the pump was equal to the ideal displacement multiplied by the pump input speed.

To this point, there are two types of methods of determining the ideal displacement of a pump. The first method determines the displacement based on the manufactured geometry of the pump and calculating the displacement of the pump. The second class of methods bases the ideal displacement on interpolated values of measured test data. These methods were developed due to the low cost of running a lab test as compared with that due to the complexity of calculating the displacement from pump internal volumes with associated manufacturing tolerances. Applying this first method to gear pumps is especially challenging. Chapter 3 of this thesis will use an interpolation method of the second class to determine ideal displacement.

2.2.1 Measurement Based Ideal Displacement

Three methods exist for determining the ideal displacement of pumps through measured test data. These methods are used to accurately estimate the displacement of the pump without precise knowledge of the construction or geometric dimensions of the components within the pump [1]. These measurement-based methods all require a set of steady state tests at specific operating conditions for interpolation of ideal displacement. The three methods are the Wilson method, the Toet method, and the ISO 8426 method.

2.2.1.1 Wilson Ideal Displacement Method

The Wilson method of determining Ideal displacement [2] uses two regressions on measured pump data. At the test temperature, the pump flow rate is measured across a range of multiple shaft speeds and pressures across the pump. Then the analysis has two steps, First, flow rate is regressed onto pressure and the

y-intercepts of the regression lines for each shaft speed are stored. In the second step, flow rate y-intercepts from the first step are regressed onto shaft speed, and the ideal (or theoretical) displacement is set equal to the slope of the regression line (Fig. 2.2).

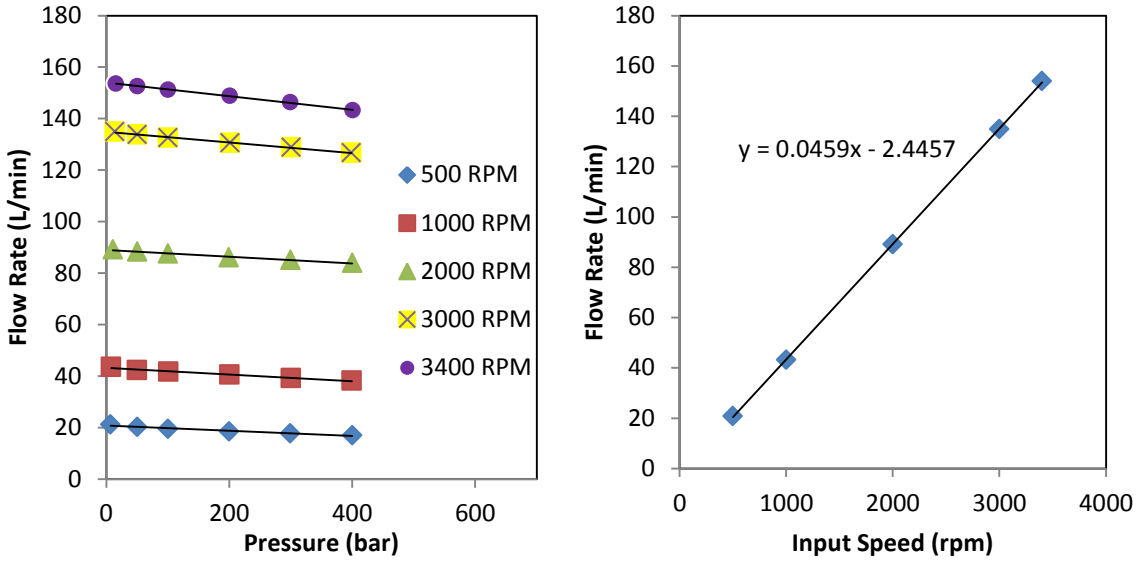

Figure 2.2. The two step process of determining ideal displacement of an axial piston pump according to the Wilson method. Step 1 of the method determines the zero crossings of the speed sub-populations (left sub-plot). In step 2, the ideal pump displacement is determined from the slope of the speed to flow points from step 1.

2.2.1.2 Toet Ideal Displacement Method

The Toet method for calculating ideal pump displacement [3] utilizes a similar method of multiple interpolations, but reverses the order to determine the ideal displacement. The first step of Toet's method is to regress the flow rate onto shaft speed for each of different test pressure difference across the pump outlet and inlet and the test temperature. The slope of each of these regression lines from the first step are then regressed against the measured pressure difference across the pump

(Fig. 2.3). The ideal displacement is set to be the x-intercept of the regression line from the second step.

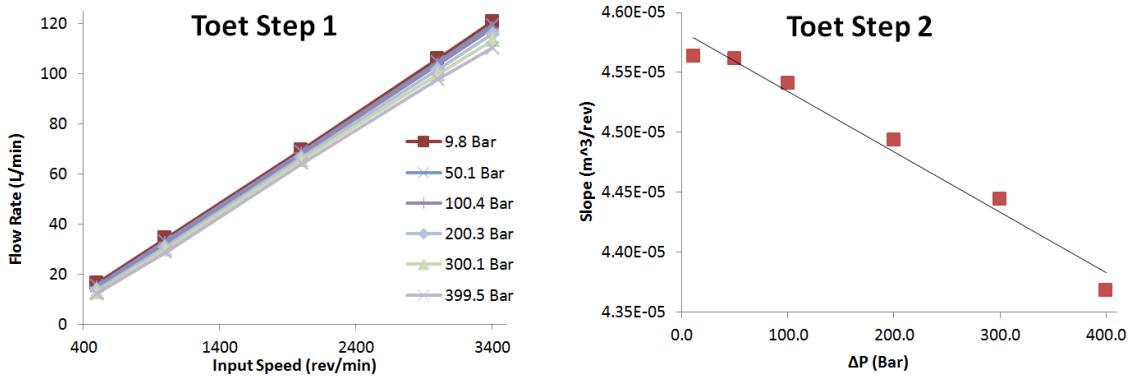

Figure 2.3. The two step process of determining ideal displacement of an axial piston pump according to the Toet method. Step 1 of the method determines the slope of the flow vs. speed regression lines for the pressure sub-populations (left sub plot). Step 2 then determines the ideal displacement from the intercept of the regressed line for the step 1 slopes and pressure points.

2.2.1.3 ISO 8426 Method

The method within ISO 8426:2008, entitled Hydraulic Fluid Power, Positive Displacement Pumps And Motors, Determination Of Derived Capacity [4], specifies that the ideal displacement is found by utilizing the slope (Fig. 2.4) of regression measured flow rate onto the measured shaft speed. These data are measured while the pump is operating at 5% of its rated pressure. Mathematically, the ideal pump displacement is set according to the relationship:

$$V_p = \left(\frac{\Delta q_{V2,e}}{\Delta n_{pump}}\right)_{p2=0.05\ p_{max},\theta} \tag{2.1}$$

where:

V_p is the ideal displacement determined at a specific temperature and 5% of rated pressure,
$\Delta q_{V2,e}$ is the average change in flow, and
Δn_{pump} is the average change in measured shaft speed.

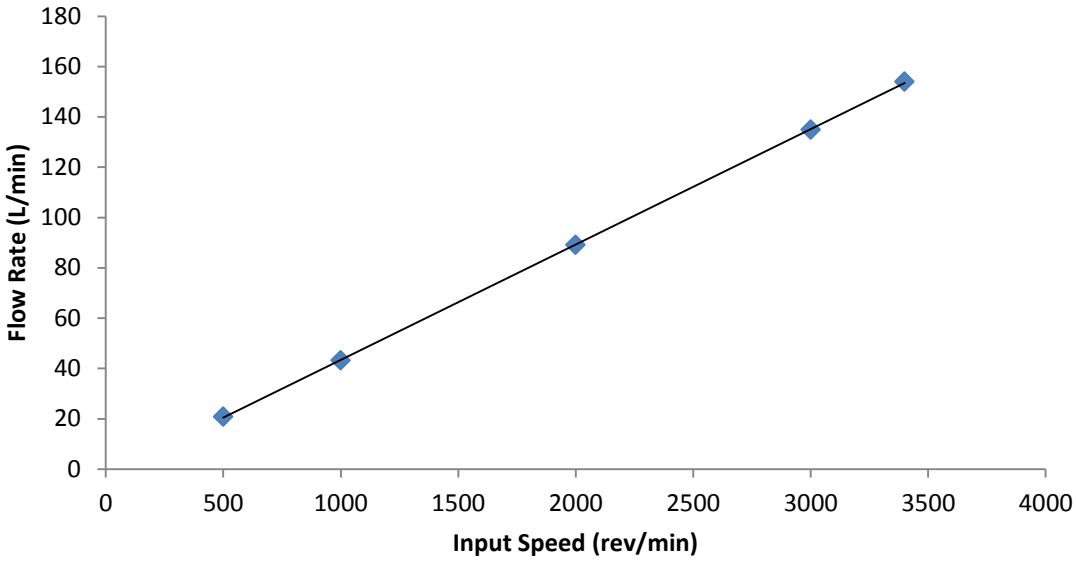

Figure 2.4. The determination of ideal pump displacement by ISO standard 8426 is accomplished by setting the ideal displacement to the slope of the regression line of flow rate as a function of pump shaft speed and 5% of rated pressure of the pump.

2.2.2 Geometric Ideal Displacement Method

A precise calculation of the ideal displacement of hydraulic pumps can be accomplished given sufficient geometric data about the displacement elements. For an axial piston pump, the ideal displacement is equal to the volume that all of the pistons sweep out during a single shaft rotation. Figure 2.5 shows a cross sectional view of the rotating group and includes depicts the dimensions needed to determine ideal displacement.

The calculation for ideal displacement of an axial piston pump described by in many textbooks, including Ivantysyn and Ivantysynova [5], and is shown mathematically to be:

$$V_p = A_{piston} H_{stroke} z \tag{2.2}$$

Where

A_{piston} is the cross sectional area of a the piston,

H_{stroke} is the total stroke length that the piston travels during a single

revolution of the input shaft, and
z is the number of pistons in the pump.

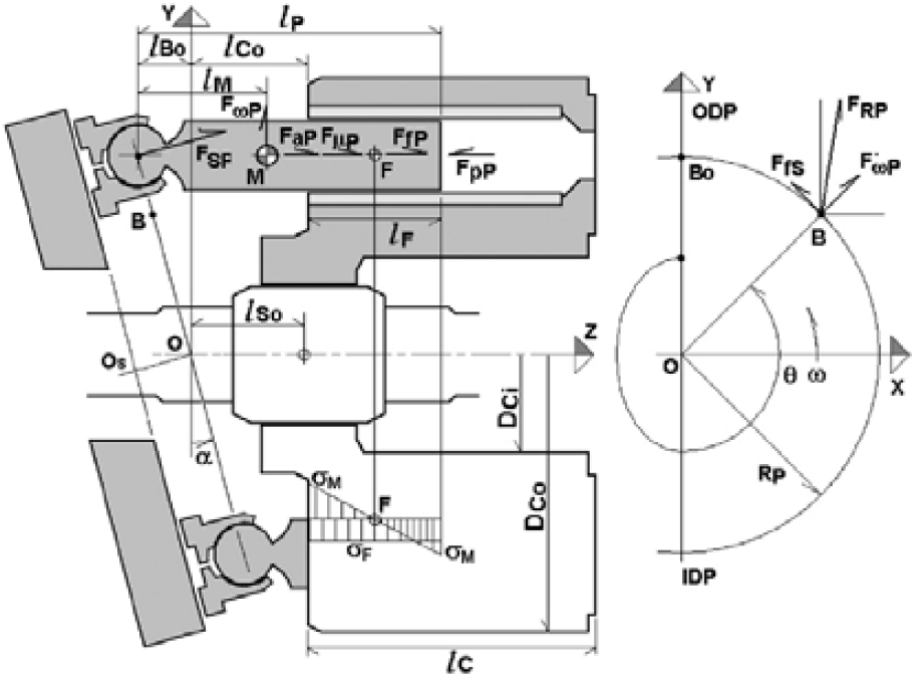

Figure 2.5. A cross sectional view of the rotating group in an axial piston pump with dimensions identified (from Jeong [19]).

The area of the piston and the stroke length are:

$$A_{piston} = \pi \left(\frac{d_{piston}}{2}\right)^2 \tag{2.3}$$

where

d_{piston} is the diameter of a piston from the rotating group, and

$$H_{stroke} = 2R_{piston} \tan(\alpha) \tag{2.4}$$

where

R_{piston} is the pitch circle radius of the pistons in the rotating group, and
α is the swash angle of the pump.

This geometric method does have a few drawbacks. Based on the variation of hardware component dimensions and any potential tolerance stack-up issues could lead to an over-estimation or under-estimation of the ideal displacement. A

displacement determination method based on measured test data is robust against making errors based on geometric relationships and tolerances of rotating group components.

2.3 Steady State Flow Loss Overview

Hydraulic pumps are designed to have some inherent loss within them. Flow losses are necessary to lubricate sliding and loaded bearing surfaces and transfer heat to ensure a long and consistent operating life of the pump. Other mechanical losses related to viscous friction on internal components rotating at input shaft speed inside the case is unavoidable. Understanding the sources of loss and quantifying them has been a topic of research dating back many decades.

In the successive portions of this thesis, a common notation for pump pressures has been adopted. Additionally, the pressures are all gage pressure, so the gauge pressure of associated with atmospheric pressure is defined to be zero. The pump pressure naming convention has five pump pressures, which are: 1) the high system pressure at the pump outlet, which is labeled p_{hp}, 2) low system pressure at the pump inlet, which is labeled p_{lp}, 3) the internal case pressure of the pump, which is labeled p_{case}, 4) atmospheric pressure, which is labeled p_{atm}, and 5) the pressure rise across the pump, which is labeled Δp_{sys}, and is the difference between p_{hp} and p_{lp} (Fig. 2.6). This common naming convention is needed to alleviate confusion between models covered in this chapter due to the variety of naming conventions used by the authors cited.

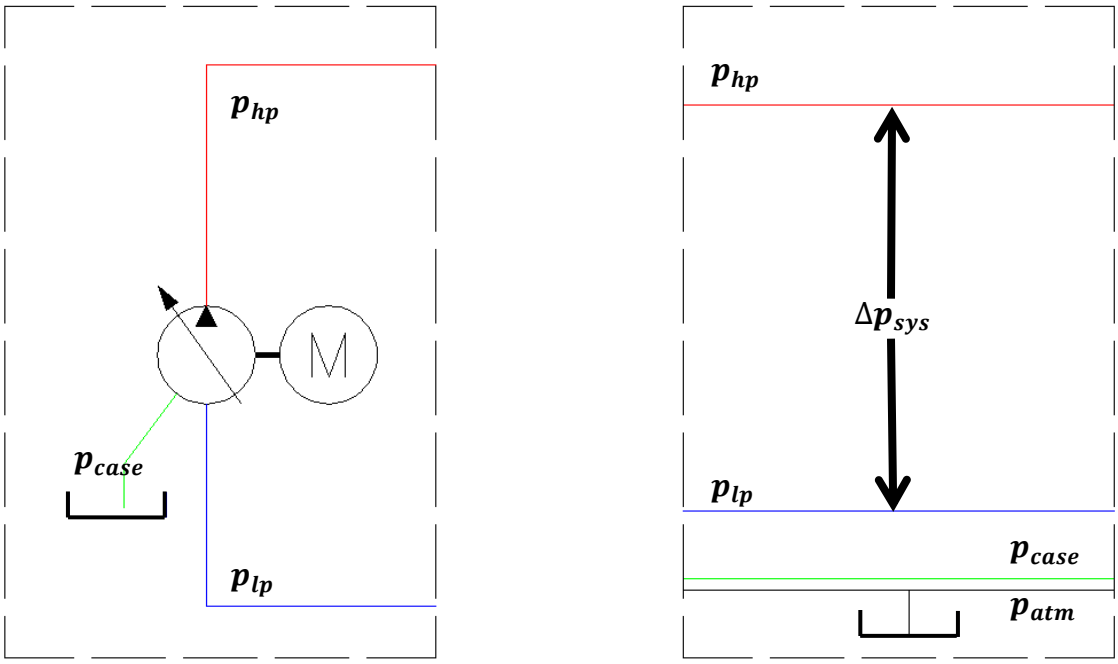

Figure 2.6. A graphical representation of the pressure naming convention used in this thesis. The left side of the figure is a schematic of a hydrostatic pump with the pressures illustrated with 1) high pressure in red, 2) charge pressure in blue, 3) case pressure in green and 4) atmospheric pressure in black. On the right is a depiction of the relative value of pressure with respect to atmospheric pressure.

An important distinction needs to be made between pump losses and pump efficiency. Rahmfeld and Meincke [6] concluded that when modeling the difference between the ideal and actual flow out of a pump, loss models should predict the flow loss and not the ratio between the measured and ideal flow. The primary advantage of this is that large modeling errors can appear to be small in the context of efficiency. In all of the flow loss models within this paper, with only a single exception, losses were considered instead of efficiency.

The definition of flow loss is the difference between the ideal flow and measured flow. Flow loss is mathematically represented as:

$$Q_L = n_{pump} V_P \varepsilon_P - Q_{Meas} \tag{2.5}$$

where:

n_{pump} is the pump input speed,

V_P is the ideal displacement of the pump,

ε_P is the percent of maximum displacement of the pump, and

Q_L is the sum of the volumetric losses of the pump.

A variety of steady state flow loss models have been developed for both hydraulic pumps and motors (Table 2.1). Each of the models can be categorized into one of three types: 1) physical models, 2) analytical models and 3) numerical models [7]. Over time, the number of parameters has generally increased to both better describe experimental data as well as model the physical processes that were understood at that time that they were published [2], [8] – [14], [5], [15] – [19].

Physical flow loss models quantify loss using terms based on physical principles of processes or component interactions. Early examples of physical models such as those described by Wilson [2], Schlösser [8] and Olsson [9] include physical processes such as laminar and turbulent flow loss. Later physical models, like those described by Bavendiek [13], Kögl [15], and Jeong [19] calculated losses as the sum of sources of interaction between moving components within the pump. Interfaces that are common between the two models are the piston to cylinder-block bore interface, the cylinder-block to valve plate interface and the piston-slipper to swash-plate interface.

Table 2.1. Summary of the steady state loss models for hydraulic pumps including the number of variables within the models.

Author	Year	Model Type	Number of Terms
Wilson	1948	Physical	2
Schlösser	1961	Physical	2
Olsson	1973	Physical	4
Pacey, Turnquist and Clark	1979	Physical	2
Zarotti and Nevegna	1981	Analytical	5
Rydberg	1983	Analytical	5
Bavendiek	1987	Physical	11
Dorey	1988	Analytical	2
Ivantysyn, Ivantysynova	1993	Numerical	27*
Kögl	1995	Physical	11**
Huhtala	1997	Numerical	12
Baum	2001	Numerical	3 layers
Ortwig	2002	Numerical	3
Jeong	2006	Physical	6

* The Ivantysyn and Ivantysynova model can vary in the number of parameters based on the maximum exponent selected.
** Huhtala parameters are based on test data at the extremes of the operating range, not based on the complete data set.

Numerical models explain the flow loss data by means of a statistical model, relating flow loss to relevant operational variables; typically pressure across the pump, shaft speed and pump displacement. The parameters within the models have little or no physical meaning, but may usefully explain the variation in the data. These models require a large number of measurements to define the loss behavior of the pump. A notable example of this type of model is that of Ivantysyn and Ivantysynova [5]. Their loss model is a linear combination of model term which are products of three system variables (pump displacement, delta pressure and shaft speed) raised to powers with exponents from zero to a desired value (typically 2 or 3). The authors suggested that a viscosity variable could also be added.

The analytical models are a blend of physical and numerical models. The majority of the terms have physical meaning, but additional terms are added to better explain variation in the data. For example, the Zarotti and Nevegna [11] added terms that had little physical meeting, but reported increased the capability of the model to explain measured test data variability.

2.4 Individual Loss Models

The authors of the models described above exhibited different motivations for developing their models. Additionally, many of the authors modeled the flow out of the pump as a difference between the ideal pump flow and flow loss. The remainder of this section will only discuss the flow loss portion of each of their models. Also, a common set of variables will be used where possible; for example, Δp_{sys} will be used to denote the pressure rise across the pump within the flow loss model.

2.4.1 Wilson Loss Model

The first mathematical pump flow loss model for hydraulic pumps is widely recognized to be developed by Wilson [2]. Wilson's flow model describes pump flow loss with laminar loss flow and constant flow loss terms. Mathematically, the model is represented by:

$$Q_L = C_S \frac{V_P \Delta p_{sys}}{2\pi\mu} + Q_{const.} \tag{2.6}$$

where

C_S is the laminar flow loss constant,
μ is the oil viscosity,
$Q_{const.}$ is the constant/ delivery flow loss parameter, and
Q_L is the total flow loss.

The justification for this relationship is that most of the flow loss is assumed to be leakage flow past the pumping elements. This leakage flow is assumed to be laminar because the clearances within a pump are quite small. The constant flow loss term models the flow losses associated with drawing the fluid into the displacement element. This constant is generally small and some subsequent authors omit the term when reviewing the model.

2.4.2 Schlösser Loss Model

Schlösser [8] built upon Wilson's models by removing the constant flow term and replacing it with a turbulent flow loss term. The flow equation was modified by replacing the constant flow loss term term with a turbulent loss term that is similar in structure to an orifice equation with the area of the orifice being proportional to the displacement volume to the two-thirds power. This addition and a subsequent better fit of data brings into question the assumption of Wilson that all flow loss is laminar. Mathematically, the Schlösser flow loss model is written as:

$$Q_L = C_S \frac{V_P \Delta p_{sys}}{2\pi\mu} + C_{st} V_P^{\frac{2}{3}} \sqrt{\frac{2\Delta p_{sys}}{\rho}} \tag{2.7}$$

where

C_{st} is the turbulent flow loss constant, and

ρ is the density of the hydraulic fluid.

2.4.3 Olsson Loss Model

Olsson [9] developed a flow loss model that introduced compressibility effects into the flow loss model. Starting with the terms from the Schlösser flow loss model, Olson added two loss terms to account for the compressibility of the pump flow. The two compressibility terms accounted for displacement independent flow loss in the

term with the coefficient, C_{C1}, and displacement dependent flow loss in the term with the coefficient, C_{C2}. This compressibility effect became evident when testing axial piston machines under high pressures compared to other types of positive displacement pumps, for example, gear pumps. For example, at 414 bar (6000 psi), a three percent compression of a petroleum-based hydraulic fluid is typical. Mathematically, the Olsson flow loss model is written as:

$$Q_L = C_S \frac{V_P \Delta p_{sys}}{2\pi\mu} + C_{sl} V_P^{\frac{2}{3}} \sqrt{\frac{2\Delta p_{sys}}{\rho}} + \left(C_{C1} - C_{C2}\varepsilon_P\right)\frac{V_P \Delta p_{sys}}{\beta_{oil}} \tag{2.8}$$

2.4.4 Pacey, Turquist and Clark Loss Model

Pacey, Turquist and Clark [10] built a flow loss model upon Wilson's model and proposed a model for both pumps and motors. The first term of their flow loss model is the same as Wilson's model with the second term accounting for viscosity based losses. Pump flow loss was described mathematically as:

$$Q_L = C_S \frac{V_P \Delta p_{sys}}{2\pi\mu} + \frac{C_{CP}}{\mu} \tag{2.9}$$

where

C_{CP} is the viscous flow loss coefficient.

2.4.5 Zarotti and Novenga Loss Model

Zarotti and Novenga [11] also studied axial piston machines and developed a model for modeling flow loss. In their flow loss model, a number of model terms explained experimental flow loss data. The pump flow loss is described mathematically as:

$$Q_L = C_1 \Delta p_{sys} + C_2 \Delta p_{sys}^2 + C_3 \Delta p_{sys}^2 n_p^{\frac{3}{2}} + C_4 \Delta p_{sys} n_n \left(C_5 + \varepsilon_P V_P\right) \tag{2.10}$$

Using their model, Zarotti and Novenga could reliably predict the behavior of a pump. Each of the model terms, apart from the compressibility and power dependent terms, have little physical meaning, yet they do aid in improving the model's capability in describing flow loss variability.

2.4.6 Rydberg Loss Model

Rydberg proposed a flow loss model [12] that built on the Olsson model and was developed specifically to model variable displacement axial piston pumps. After studying the models developed by many of the proceeding authors, Rydberg concluded that a model that could explain 98% of the measured variability in the flow loss would require physical terms as well as higher order terms. Based on this strategy, he developed the Rydberg flow loss model, which is written mathematically as:

$$Q_L = a_o \varepsilon_P V_P n_P + (a_1 + a_2 \varepsilon_P) \frac{V_P n_P \Delta p_{sys}}{\beta} + a_{3_P} \frac{V_P \Delta p_{sys}}{2\pi\mu} + a_4 V_P \Delta p_{sys}^2 \qquad (2.11)$$

where

a_o is the flow dependent coefficient,
$a_1$is the displacement setting independent compressibility loss coefficient,
$a_2$is the displacement setting dependent compressibility loss coefficient,
a_3 is the laminar flow loss coefficient, and
a_4 analytical loss coefficient (best fit for axial piston pumps).

2.4.7 Bavendiek Loss Model

The Bavendiek flow loss model [13] departs from the previous physical models because the loss terms are derived component interaction level flow losses instead of a system level flow loss terms. For example, in the Wilson loss model, laminar flow loss is a represented with a single term, but Bavendiek initially modeled viscous flow losses in several interfaces among them is the piston seal to cylinder-

block bore interface. Then for convenience, Bavendiek reduced similar terms within the loss models, and replaced gap heights and flow coefficients with lumped parameters. Bavendiek considered five sources or interactions that produced flow losses in a bent axis motor. The five flow loss locations include (Figure 2.7): 1) the leakage between the piston and the cylinder-block bore (in the rotating group), 2) piston ball and retainer (between the rotating group and shaft), 3) piston and piston rod, 4) swash block and the cylinder-block running face, and 5) swash block lubrication notches. To complete the loss model, a fluid compressibility loss term was added.

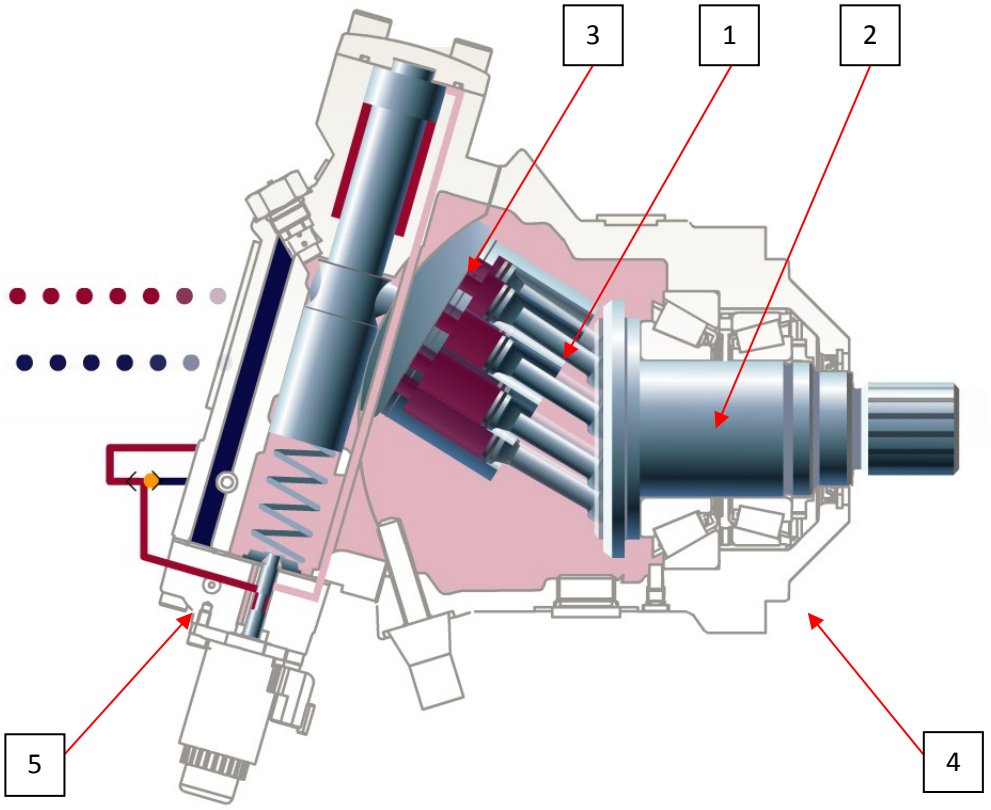

Figure 2.7. Components of a bent-axis piston motor. 1) rotating group, 2) output shaft 3) swash-block, 4) housing, 5) end-cap (courtesy Danfoss Power Solutions).

The Bavendiek flow loss model is written mathematically as:

$$Q_{LM} = Q_{L1} + Q_{L2} + Q_{L3} + Q_{L4} + Q_{L5} + Q_{L6} + Q_{L7} + Q_{L8} + Q_{L\_COMP} \tag{2.12}$$

where

Q_{LM} is the total flow loss for a motor,

Q_{L1} is the high pressure squared dependent loss term, and is represented mathematically by:

$$Q_{L1} = K_1 \frac{\Delta p_{sys}\, V_{max}}{\mu} \left(\frac{p_{hp}}{p_{case}}\right) \tag{2.13}$$

Q_{L2} is the high pressure cubed dependent loss term, and is represented mathematically by:

$$Q_{L2} = K_2 \frac{\Delta p_{sys}\, V_{max}}{\mu} \left(\frac{p_{hp}}{p_{case}}\right)^2 \tag{2.14}$$

Q_{L3} is the high pressure to the fourth power loss term, and is represented mathematically by:

$$Q_{L3} = K_3 \frac{\Delta p_{sys}\, V_{max}}{\mu} \left(\frac{p_{hp}}{p_{case}}\right)^3 \tag{2.15}$$

Q_{L4} is charge pressure dependent loss term, and is represented mathematically by:

$$Q_{L4} = K_4 \frac{\left(p_{lp} - p_{atm}\right) V_{max}}{\mu} \tag{2.16}$$

Q_{L5} is the charge pressure square root dependent loss term, and is represented mathematically by:

$$Q_{L5} = K_5 \sqrt{\frac{\left(p_{lp} - p_{atm}\right)}{\rho}}\, V_{max}^{\frac{2}{3}} \tag{2.17}$$

Q_{L6} is the loss term that is dependent on the product of delta pressure and shaft speed, and is represented mathematically by:

$$Q_{L6} = K_6 \frac{\alpha}{\alpha_{max}} V_{max}\, n \left(\frac{p_{hp}}{p_{case}}\right) \tag{2.18}$$

Q_{L7} is the loss term with linear dependency on delta pressure, and is represented mathematically by:

$$Q_{L7} = K_7 \frac{\Delta p_{sys}\, V_{max}}{\mu} \tag{2.19}$$

Q_{L8} is the delta pressure square root dependent loss term, and is represented mathematically by:

$$Q_{L8} = K_8 \sqrt{\frac{\Delta p_{sys}}{\rho}}\, V_{max}^{\frac{2}{3}} \tag{2.20}$$

Q_{L_COMP} is the bulk modulus flow loss term, and is represented mathematically by:

$$Q_{L\_COMP} = K_9\, z\, n\, \beta\, \Delta p_{sys}\, V_{Z\_COMP} \tag{2.21}$$

The model coefficients K_1 through K_9 were selected using an optimization algorithm called GLGOPT that Bavendiek used to minimize the error between the measured and modeled flow loss.

2.4.8 Dorey Loss Model

Dorey [14] proposed a number of steady-state models for a number of different designs of pumps and motors, including a flow loss model developed for variable displacement pumps specifically is shown in equation 2.22. The model includes a non-linear leakage term as well as losses due to compression of fluid. The Dorey flow loss model is written mathematically as:

$$Q_P = \varepsilon_P V_P n_P - C_s^* \frac{V_P \Delta p_{sys}}{2\pi\mu} - \frac{\Delta p_{sys} n_p V_p}{\beta}\left(V_r + \frac{1+\varepsilon_p}{2}\right) \tag{2.22}$$

where

C_s^* is the non-linear, laminar leakage coefficient,

$$C_s^* = C_s\left(\frac{\Delta p_{sys}}{p_{case}}\right)\left(a + b\frac{n}{n_{\max}}\right), \tag{2.23}$$

a is the pressure dependent constant within the laminar leakage coefficient,

b is the pressure and flow dependent constant within the laminar leakage coefficient, and

V_r is the ratio between the dead volume of the axial piston rotating group and displacement V_p.

2.4.9 Ivantysyn and Ivantysynova Loss Model

Ivantysyn and Ivantysynova [5] developed a flow loss model that is a statistical power model using three primary system variables for pumps: pressure across the pump, shaft speed and displacement. The Ivantysyn and Ivantysynova flow loss model is written mathematically as:

$$Q_s = \sum_{i=0}^{p}\sum_{j=0}^{q}\sum_{k=0}^{r} k_{ijk}\, V^i n^j \Delta p_{sys}{}^k \tag{2.24}$$

The motivation for this model was to mathematically describe the flow loss as a function of system variables without concern of the source of the loss. With the inherent complex nature of flow loss, Ivantysyn and Ivantysynova argue that the exact sources of loss and the underlying physics need not be understood to obtain accurate loss models.

The model order is determined by the terms *p*, *q* and *r*, which not only change the number of terms within the model, but also change the power of the system variables within a term. Generally, a maximum power of two is initially used then the model coefficients are found using a numerical method or technique (ordinary least squares linear regression will be used in this work). In the paper describing this model, the authors commented that hydraulic viscosity could be used as a fourth system variable in the model.

2.4.10 Kögl Loss Model

The Kögl flow loss model [15] emerged in a similar manner to the Bavendiek model. Both model are based on first-principle loss models and are then simplified to a model with lumped terms multiplied by model coefficients. The primary

difference between the two is that the Kögl model was developed to describe losses with terms based on axial piston pumps where the Bavendiek model was developed for bent-axis motors. The component interfaces that Kögl identified as likely sources of flow loss are: 1) the cylinder-block to valve-plate interface, 2) the cylinder-block bore to piston interface, 3) the piston to slipper interface, and 4) the slipper to swash-plate interface. The model also accounts for losses to control the pump and fluid compressibility. Kögl, like Bavendiek, derived the flow loss model as the sum of the losses from individual locations of interaction and then collected like terms. The Kögl flow loss model is written mathematically as:

$$Q_{LP} = Q_{L1} + Q_{L2} + Q_{L3} + Q_{L4} + Q_{L5} + Q_{L6} + Q_{L7} + Q_{L8} + Q_{L9} + Q_{L10} + Q_{L11} \quad (2.25)$$

where

Q_{L1} is the laminar flow loss between the piston and cylinder-block due to the system pressure delta and is represented mathematically by:

$$Q_{L1} = K_{Q1} \frac{\Delta p_{sys} V_{max}}{\eta_o} \quad (2.26)$$

Q_{L2} is the laminar flow loss between the piston and cylinder-block due to the pressure drop between charge pressure and case pressure and is represented mathematically by:

$$Q_{L2} = K_{Q2} \frac{\left(p_{lp} - p_{case}\right) V_{max}}{\eta_o} \quad (2.27)$$

Q_{L3} is the laminar flow loss between the piston and cylinder-block due to the linear relationship between high pressure and case pressure by:

$$Q_{L3} = K_{Q3} \frac{\Delta p_{sys} V_{max}}{\eta_o} \left(\frac{p_{hp}}{p_{case}}\right) \quad (2.28)$$

Q_{L4} is the laminar flow loss between the piston and cylinder-block due to the squared relationship between high pressure and case pressure by:

$$Q_{L4} = K_{Q4} \frac{\Delta p_{sys} V_{max}}{\eta_o} \left(\frac{p_{hp}}{p_{case}}\right)^2 \quad (2.29)$$

Q_{L5} is the laminar flow loss between the piston and cylinder-block due to the cubic relationship between high pressure and case pressure by:

$$Q_{L5} = K_{Q5} \frac{\Delta p_{sys} V_{max}}{\eta_o} \left(\frac{p_{hp}}{p_{case}}\right)^3 \quad (2.30)$$

Q_{L6} is the laminar flow loss for the slipper that is linearly dependent on the ratio between actual and rated shaft speed by:

$$Q_{L6} = K_{Q6} \frac{\left(\Delta p_{sys} + p_{lp} - p_{case}\right) V_{max}}{\eta_o} \left(\frac{n}{n_{ref}}\right) \quad (2.31)$$

Q_{L7} is the laminar flow loss for the slipper that has a squared relationship between actual and rated shaft speed by:

$$Q_{L7} = K_{Q7} \frac{\left(\Delta p_{sys} + p_{lp} - p_{case}\right) V_{max}}{\eta_o} \left(\frac{n}{n_{ref}}\right)^2 \quad (2.32)$$

Q_{L8} is the laminar flow loss for the slipper that has a cubic relationship between actual and rated shaft speed by:

$$Q_{L8} = K_{Q8} \frac{\left(\Delta p_{sys} + p_{lp} - p_{case}\right) V_{max}}{\eta_o} \left(\frac{n}{n_{ref}}\right)^3 \quad (2.33)$$

Q_{L9} is the turbulent flow loss for the valve-plate dependent on high system delta pressure by:

$$Q_{L9} = K_{Q9} V_{max}^{\frac{2}{3}} \sqrt{\frac{\Delta p_{sys}}{\rho}} \quad (2.34)$$

Q_{L10} is the turbulent flow loss for the valve-plate dependent on pressure drop from charge pressure to case pressure by:

$$Q_{L10} = K_{Q10} V_{max}^{\frac{2}{3}} \sqrt{\frac{p_{lp} - p_{case}}{\rho}} \quad (2.35)$$

Q_{L11} is the fluid compressibility loss related to the dead-volume in the rotating group by:

$$Q_{L11} = K_{Q11} V_{max} \beta n \Delta p_{sys} \quad (2.36)$$

Q_{L12} is the fluid compressibility loss related to the displaced volume of the rotating group by:

$$Q_{L12} = K_{Q11} V_{max} \frac{tan(\alpha)}{tan(\alpha_{max})} \beta n \Delta p_{sys} \quad (2.37)$$

2.4.11 Huhtala Loss Model

Huhtala [16] developed a flow loss model for a hydrostatic transmission consisting of a single pump and a single motor. The goal for the model derivation was to achieve an “acceptable” accuracy with a “reasonable” amount of data. Huhtala’s approach to develop the model was to identify the maximum and minimum speeds and pressures at which the pump operated. Then two curves (or two lines) were generated from flow loss measurements acquired at regular pressure intervals at the maximum and minimum rated shaft speeds. Curves were fit to the flow loss – pressure data. These curves were represented by the functions $q_{n,max}(p)$ and $q_{n,min}(p)$ which were at the maximum and minimum pump shaft speeds, respectively (Figure 2.8).

A similar procedure was then carried out by generating curve fits of flow loss as a function of shaft speed at the maximum and minimum pump pressures. The functions, $Q_{Pmax}(n)$ and $Q_{Pmin}(n)$, represent the relationship between flow loss and shaft speed at the maximum and minimum pressures, respectively.

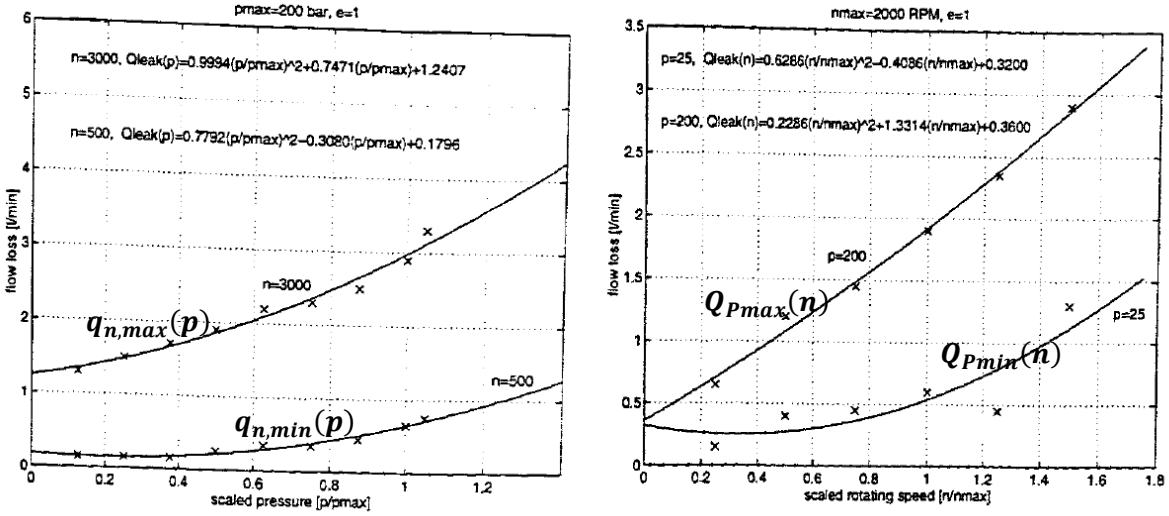

Figure 2.8. A plot of the polynomial fit to find the "two line" curves for the flow loss of an axial piston pump. The left plot is determining the equations $q_{n,max}(p)$ and $q_{n,min}(p)$ with the right determining $Q_{Pmax}(n)$ and $Q_{Pmin}(n)$. (From Huhtala [16]).

The pump flow loss in the Huhtala model is the theoretical pump flow less a pressure and speed dependent flow loss term $Q_{v_{n,p}} f_v(\varepsilon)$, a viscosity dependent flow loss term $f_v(\mu)$, and a bulk modulus flow loss term $f_v(\beta)$. All three terms are generated through the methodology described above. Thus the flow loss is represented mathematically as:

$$Q_L = \left(Q_{v_{n,p}} f_v(\varepsilon) + f_v(\mu) + f_v(\beta)\right), \tag{2.38}$$

where,

$Q_{v_{n,p}}$ is the pressure and speed dependent flow loss, and mathematically is:

$$Q_{v_{n,p}} = \left(Q_{Pmax}(n) - Q_{Pmin}(n)\right)\left(\left(q_{n,max}(p) - q_{n,min}(p)\right)\left(\frac{n-n_{min}}{n_{max}-n_{min}}\right) + q_{n,min}(p)\right) + Q_{Pmin}(n), \tag{2-39}$$

$Q_{Pmax}(n)$ is the speed dependent flow loss rate at maximum pressure equation,

$Q_{Pmin}(n)$ is the speed dependent flow loss rate at minimum pressure equation,
$q_{n,max}(p)$ is the pressure dependent flow loss rate at maximum pressure equation,
$q_{n,min}(p)$ is the pressure dependent flow loss rate at minimum pressure equation,
n_{max} is the maximum shaft speed,
n_{min} is the minimum shaft speed,
$f_v(\varepsilon)$ is the displacement setting dependent flow losses, and mathematically is:

$$f_v(\varepsilon) = \left(f_{Pmax}(\varepsilon) - f_{Pmin}(\varepsilon)\right)\left(\frac{p-p_{min}}{p_{max}-p_{min}}\right) + f_{Pmin}(\varepsilon), \quad (2.40)$$

$f_{Pmax}(\varepsilon)$ is the displacement dependent flow loss rate at maximum pressure equation,
$f_{Pmin}(\varepsilon)$ is the displacement fitted flow loss rate at maximum pressure equation,
p_{max} is the maximum pressure in the measured data set,
p_{min} is the minimum pressure in the measured data set,

$f_v(\mu)$ is the viscosity dependent flow losses, and mathematically is:

$$f_v(\mu) = \left(f_{\mu max}(p) - f_{\mu min}(p)\right)\left(\frac{\mu-\mu_{min}}{\mu_{max}-\mu_{min}}\right), \quad (2.41)$$

$f_{\mu max}(p)$ is the pressure dependent flow loss rate at maximum viscosity equation,
$f_{\mu min}(p)$ is the pressure dependent flow loss rate at minimum viscosity equation,
μ_{max} is the maximum viscosity in the measured data set,
μ_{min} is the minimum viscosity in the measured data set,
$f_v(\beta)$ is the bulk modulus dependent flow losses, and mathematically is:

$$f_v(\beta) = p_P n_P V_P \left(V_r + \frac{1+\varepsilon_P}{2}\right)\left(\frac{1}{\beta} - \frac{1}{\beta_{fit}}\right), \text{ and} \quad (2.42)$$

β_{fit} is the bulk modulus at the point that is being fitted.

2.4.12 Baum Loss Model

Baum [17] investigated the use of artificial neural networks (ANN) to describe efficiency of hydrostatic units. The Baum ANN model was constructed with an three element input layer and a three element hidden layer and connected by synapses

and an outer layer connected to the hidden layer with neurons with two outputs of volumetric efficiency (Fig. 2.9). The model was developed for a particular pump through a training the ANN with the back-propagation process that varies the strength of each of the synapses and compares the output value to the measured efficiency.

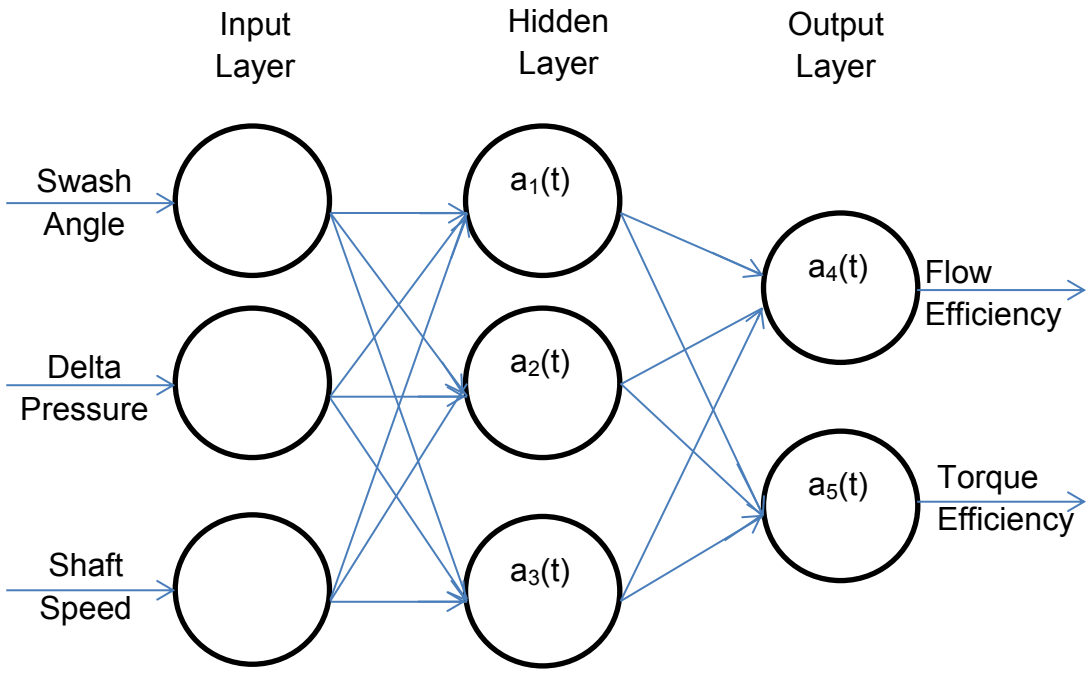

Figure 2.9. A graphical representation of the Baum flow efficiency. This neural network is constructed with an input layer, a hidden layer and an output layer.

2.4.13 Ortwig Loss Model

Ortwig [18] developed a flow loss model similar to the Ivantysyn and Ivantysynova model by virtue of the fact that both models are calibrated to test data without attempting to model particular physical phenomena. The goal of the model was to accurately model the measured data with the least number of model terms as possible. The Ortwig flow loss model was developed starting with a numerical expansion similar to the Ivantysyn and Ivantysynova model with the maximum

exponents of 1, 1, and 3 for displacement, pump input speed and pressure across pump variables respectively; yielding sixteen terms. Model coefficients were determined using least squares linear regression across a wide range of pumps and motors.

The Ortwig flow loss model determined the first three model terms using the methodology above. When the model consisting of the first three terms was validated, the error between the measured data and modeled flow loss was high at low shaft speeds and small swash-plate angle. To correct this, a fourth term was added with exponential terms that become large at these low speed and angle conditions. This model term addition yielded an error over the measured operating range to less than 10%.

$$Q(\alpha, n, \Delta p) = q_1\, \alpha\, n + q_2\, n\, \Delta p_{sys} + q_3\, \Delta p_{sys} + q_4\, e^{\left(\frac{-\alpha}{K_\alpha}\right)}\, e^{\left(\frac{-n}{K_n}\right)} \tag{2.43}$$

2.4.14 Jeong Loss Model

Jeong [19] developed a motor loss model similar to the Bavendiek and Kögl models. All three models attempt to capture losses based on a first-principle understanding of the closed circuit axial piston machines. Many of the terms among the three models are similar, but the Jeong model had a number of simplifying assumptions that resulted in a model with a lower number of terms.

In the papers documenting the Jeong model, the flow loss was stated to be the sum of seven physical loss terms. Those terms included: 1) the flow loss between the pistons and the cylinder block, 2) the flow loss between the slippers and the swash-plate, 3) the flow loss between the valve-plate and the cylinder-block, 4) the flow loss related to the valve-plate transition notches, 5) the flow loss due to

turbulent filling, 6) the flow loss due to fluid compressibility, and 7) constant flow losses.

However, a number of the model terms from the complete model were observed to be perfectly collinear with one another. For example, three interfaces within the model were observed to have a collinear laminar flow loss term: 1) the pistons and the cylinder block interface, 2) the slipper and the swash-plate interface, 3) the valve-plate and the cylinder-block interface. These terms were grouped into a single laminar flow loss term. Based on this methodology of grouping similar terms, the final Jeong flow loss model consisted of model terms that represented: 1) laminar flow loss, 2) Couette flow from sliding components 3) turbulent loss due to the valve plate transition notches 4) turbulent flow loss due to rotating group filling, 5) fluid compressibility, and 6) constant leakage.

$$Q_L = C_{\mu PSV}\frac{\Delta p_{sys}}{\mu} + C_{vPV} n_{pump} + C_{VN}\sqrt{\frac{\Delta p_{sys}}{\rho}} + C_{PP}\frac{\rho n^3}{\Delta p_{sys}} + C_{\beta} n_{pump}\Delta p_{sys} + Q_{Lo} \quad (2.44)$$

2.5 Flow Loss Model Discussion

In this section, the models introduced above will be further discussed and compared with one another. The model discussion will be organized according to within the three model classes, physical, analytical and, numerical, which were introduced above.

The physical model class can be further divided into two sub-classes: 1) process-based models and 2) component interaction-based models. This division clarifies the division between the models that calculate losses with respect to the

complete pump (process-based) versus the models explain loss due to component interactions within the pump (component interaction-based).

2.5.1 Physical Process-Based Flow Models

All of the early physical flow models generally built successively on new knowledge and described more variability in flow loss. Below is a summary of the type of flow loss terms associated with each of the models (Table 2.2).

Table 2.2. Summary of the physical process based flow models. The dot indicates the presence of that type of term within the flow loss model.

Loss Source	Wilson	Schlösser	Olsson	Pacey, Turnquist, and Clark
Laminar	●	●	●	●
Turbulent		●	●	
Constant	●			
Viscous				●
Bulk Modulus (Dead Volume)			●	
Bulk Modulus (Disp. Volume)			●	

Wilson originally postulated that most of the flow losses within hydraulic pumps and motors were laminar in nature with remainder being constant. He made this assumption because of the small clearances between moving components and the resulting small Reynolds number. Building on Wilson's original model, Schlösser proposed that that some portion of the flow losses in a pump or motor are turbulent in nature.

Olsson used the Schlösser flow loss model as a starting point, and then added two additional terms to account for losses due to fluid compression in the dead volume and the displacement volume of the pump/motor. Pacey, Turnquist and Clark expanded on the original Wilson model by removing the constant loss term and adding a viscous loss term that is dependent only on viscosity.

2.5.2 Physical Component Interaction-Based Flow Loss Models

The component interaction-based flow loss models differ from the earlier flow loss model in that they model the individual sources of loss within specific types of piston machines. For example, the Bavendiek, Kögl, and Jeong models approximated the losses in a bent axis motor, a axial piston pump and an axial piston motor, respectively. Jeong did not cite either Kögl or Bavendiek in the articles documenting his model development, but instead based its development primarily on the sum of loss equations described by Ivantysyn and Ivantysynova [5].

Only the piston to cylinder-block interface is common between all three flow loss models. From there, there is some divergence, but typically, the remaining terms that model laminar or turbulent leakage paths.

Table 2.3. Summary of the physical, component interaction-based flow loss sources. The dot indicates that the component interface is included within the derivation of the flow loss model.

Loss Source	Bavendiek	Kögl	Jeong
Cylinder Block to Swash-Block Interface	●		
Cylinder-Block to Valve-Plate Interface		●	●
Cylinder Block to Piston Interface	●	●	●
Piston to Slipper Interface		●	●
Piston to Piston Rod Interface	●		
Piston-Rod Drive Flange	●		
Shaft Bearings	●		
Slipper to Swash-Plate Interface		●	
Shaft Seal	●		
Control Losses		●	
Cylinder-Block bore to Valve-Plate Kidney			●
Valve-Plate pre-compression notches			●

Bavendiek evaluated the performance of his flow loss model on four different bent-axis motors (Hydromatik A6V 164 cm^3/rev and 250 cm^3/rev, a Volvo V11 130 cm^3/rev and a Linde BMV 260 cm^3/rev). Only 27 flow loss measurements were used

to calibrate the coefficient values for each of the four motors. All four of the motors' flow loss models were calibrated in both pumping and motoring modes. Across the four devices, model performance in explaining flow loss varied with the following standard error of each of the motors: 1) 0.708 L/min. for the Hydromatik A6V 164 cm^3/rev motor, 2) 0.643 L/min. for the Hydromatik A6V 250 cm^3/rev motor, 3) 1.110 L/min. for the Volvo V11 130 cm^3/rev motor and 4) 1.07 L/min. for the Linde BMV 260 cm^3/rev motor.

The Kögl model was evaluated using a 71 cm^3/rev open-circuit axial-piston pump (model A4VSO, Rexroth, Lohr am Main, Germany). Twenty-seven data points were used to calibrate the flow loss models across all combinations of three pressures, three shaft speeds, three swash-plate angles. With the full flow loss model, the standard error of calibration of flow loss was 0.624 L/min with a maximum pump output flow of 106.5 L/min.

After calibrating the Jeong flow loss model with a least squares regression method, the model performance had a maximum efficiency error of 2.33% and an average efficiency error of 0.3% (Figure 2.10). Compared to the previous research, in which authors used very small sets of measurement data, Jeong used 311 data points to determine the parameter values within the flow loss model. The test unit for this model was a 45 cm^3/rev open-circuit axial-piston unit (model A10VM, Rexroth Lohr am Main, Germany).

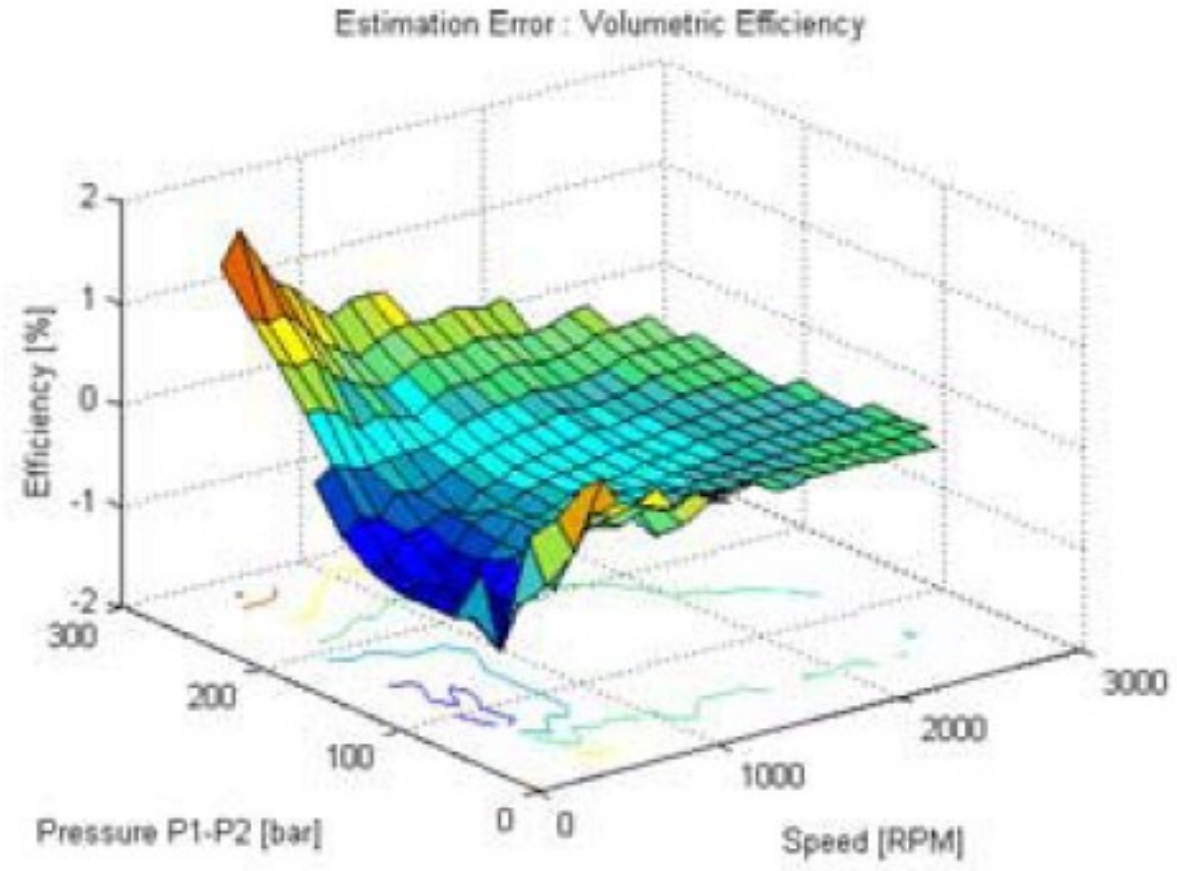

Figure 2.10. Surface plot of the volumetric efficiency estimation error as a function of pressure and speed for an axial piston motor (from Jeong [19]).

2.5.3 Analytical Flow Loss Models

The analytical flow loss models described measured data without being constrained to directly model physical processes. The terms within the models were similar to previously proposed physical models, but non-linear terms were also included in the loss models (Table 2.4).

Table 2.4. Summary of the analytical flow loss models.

Author	Flow Loss Source
Zarotti and Nevegna	Five terms, tailored to piston pumps
Rydberg	Five terms
Dorey	1) Laminar, 2) Non-linear Bulk Modulus

The Zarotti and Nevegna model was the first flow loss model to stray from the Wilson's approach of constructing a flow loss model as a sum of physical phenomena losses. In contrast, the Zarotti and Nevegna model used terms that best explained the test data. In addition, the model was developed to best describe variable displacement axial piston units compared to other models that were developed to fit many different types of units. The primary finding of Zarotti and Nevegna's work is that models with non-linear relationships to system variables calibrate to loss data better than models with linear relationships.

The Rydberg model was inspired by the Wilson and Olsson Models. The first two terms described the laminar leakage flows, and the final two terms explained the losses due to fluid compression. A goal of a ±2% maximum efficiency error over eight flow loss measurements (four speeds and two pressures) was set for the study. The measurements came from the technical literature for a 70 cc axial piston pump (model Series 22, Sauer-Sundstrand, Ames, Iowa). The Rydberg model had a maximum calibration error of 0.5% for volumetric efficiency. This accuracy was a large improvement over Wilson's model with all parameters found using linear regression.

The Dorey flow model was developed as a direct improvement of the original terms of the Wilson model. The improvement comes from replacing the constant term of the Wilson model with a function. This function added a non-linear relationship between pressure and speed to the model. Examining a number of different pump designs, Dorey concluded that this non-linear coefficient modeling approach increased the accuracy of the model compared to Wilson. This

comparison was presented through a visual comparison of flow loss for each of the measured data points. A numerical comparison of flow loss error was not presented.

2.5.4 Numerical Flow Loss Models

The Ivantysyn and Ivantysynova flow loss model, as implemented in the Polymod software application (Purdue University, West Lafayette, IN), was developed to provide a flow loss model that modeled the measured data as closely as possible (Table 2.5). As a departure from many other authors, the model did not employ any physical process, but instead took a statistical power modeling approach. The original work cited did not explicitly compare model accuracy to other models, but others have and this work will do so as well. One noted comparison was graphically depicted by Kohmäscher et. al. [7]. Their findings suggested that Polymod was quite accurate throughout the operating range, but had more error than the Huhtala model at low pump displacements.

Table 2.5. Summary of the numerical flow loss models.

Author	Flow Loss Sources
Ivantysyn, Ivantysynova	Statistical Power Model (from 27 to 125 terms)
Huhtala	1) Power dependent , 2) Viscosity dependent , 3) Bulk Modulus dependent
Baum	Three Layer Neural Network
Ortwig	Four Terms (1-3 through expansion; 4 to fit low shaft speeds)

The Huhtala flow loss models were developed to estimate the error at the limits of the operating range and interpolate data within the operating range. This model was compared to the Wilson models, and two variations of the Dorey models.

The Baum model utilized artificial neural networks to estimate the flow losses for a pump or motor. The method relies heavily on having a comprehensive data set to “teach” the loss behavior to the model. Baum attempted no direct comparison to any other flow loss models. However, Kohmäscher et. al. [7] found that the Baum model explained variation in flow loss data well, but noted that tuning of the network behavior was quite labor intensive. Additionally, just outside of the bounds of the calibration data set, unexpected model output results were observed.

The Ortwig flow loss model started using a power model and reduced it to terms that were consistently dominant across several pumps. The error between the measured and modeled flow loss was less than $\pm$10% across the entire operating range captured with 180 operating points.

2.6 CONCLUSIONS

In conclusion, a wide variety of approaches have been taken to model flow losses in axial piston pumps. Many of the models have attempted to explain variation in measured flow loss data with terms based on physical loss terms, terms assembled only to fit the data set and a blend of the two. Generally, the number of terms has increased over time as the understanding of flow losses in pumps has increased.

Many of the models present comparisons to previous author’s models and generally show an improvement with the newly developed model. However, the approaches for calibrating the models and the differing data sets used for the calibrations make it difficult to compare model performance across the available

models. The approach in Chapter three provides a clear framework for flow loss model comparison.

REFERENCES

[1] Post, W. J., 1997, “Models for steady-state performance of hydraulic pumps: determination of displacement,” Ninth International Fluid Power Workshop, Bath University, pg. 339-353.

[2] Wilson, W., 1948, “Performance criteria for positive displacement pumps and fluid motors,” ASME Semi-annual Meeting, paper No. 48-SA-14.

[3] Toet, G., 1970, “Die Bestimmung des theoretischen Hubvolumensvon hydrostatischen erdrängerpumpen und Motoren aus volumetrischen Messungen,” Ölhydraulik und Pneumatik O+P, 14 (1970) No. 5, pp. 185-190.

[4] International Standards Orginazation, 2008, “ISO 8426:2008 Hydraulic fluid power -- Positive displacement pumps and motors -- Determination of derived capacity.”

[5] Ivantysyn J. and Ivantysynova M., 2000, “Hydrostatic Pumps and Motors, Principals, Designs, Performance, Modeling, Analysis, Control and Testing,” New Delhi: Academia Books International.

[6] Rahmfeld, R. and Meincke, O., 2006, “Dynamic Simulation with Test Verification for Solving and Understanding Fluid Power System Problems,” 2nd International Conference on Computational Methods in Fluid Power, FPNI 2006.

[7] Kohmäscher, T., Rahmfeld, R., Murrenhoff, H., Skirde, E., 2007, “Improved loss modelingof hydrostatic units – requirement for precise simulation of mobile working machine drivelines,” 2007 Proceedings of ASME International Mechanical Engineering Congress and Exposition, Paper 41803.

[8] Schlösser, W., 1961, “Mathematical model for displacement pump and motors,” Hydraulic power transmission, April 1961, pp. 252-257.

[9] Olsson, O., 1973, “Matematisk verkingsgradmodell (Mathematicalv Efficiency Model), Kompendium i Hydraulik” LiTHIKP, Institute of Technology, Linköping, Sweden.

[10] Pacey, D.A., Turnquist, R.O. and Clark, S.J., 1979, “The Development of a Coefficient Model for Hydrostatic Transmissions,” 35th National Conference in Fluid Power, Chicago, IL, USA, pp. 173-178.

[11] Zarotti, L. and Nevegna, N., 1981, “Pump Efficiencies Approximation and Modeling,” 6th International Fluid Power Symposium, Cambridge, UK.

[12] Rydberg, K.-E., 1983, “On performance optimization and digital control of hydrostatic drives for vehicle applications,” Linköping Studies in Science and Technology, Dissertation No. 99, Linköping.

[13] Bavendiek, R., 1987, “Verlustkennwertbestimmung am Beispiel von hydrostatischen Maschinen in Schrägachsenbauweise” Doctoral thesis, VDI Fortschrittsberichte, Reihe 7 Nr. 122, VDI Verlag.

[14] Dorey, R., 1988, “Modelling of losses in pumps and motors,” 1st Bath International Fluid Workshop, University of Bath.

[15] Kögl, C., 1995, “Verstellbare hydrostatische Verdrängereinheiten im Drehzahl- und Drehmomentregelkreis am Netz mit angepasstem Versorgungsdruck,” Doctoral thesis, Institut für fluidtechnische Antriebe und Steuerungen IFAS, RWTH Aachen.

[16] Huhtala, K., 1996, “Modelling of Hydrostatic Transmission – Steady State, Linear and Non-Linear Models,” Mechanical Engineering Series No. 123, Tampere.

[17] Baum, H., 2001, “Einsatzpotentiale neuronaler Netze bei der CAE-Tool unterstützten Projektierung fluidtechnischer Antriebe” Doctoral thesis, Institut für fluidtechnische Antriebe und Steuerungen IFAS, RWTH Aachen.

[18] Ortwig, H., 2002, “New Method of Numerical Calculation of Losses and Efficiencies in Hydrostatic Power Transmissions” SAE International Off-Highway Congress, Las Vegas, NV.

[19] Jeong, H., 2007. “A Novel Performance Model Given by the Physical Dimensions of Hydraulic Axial Piston Motors: Model Derivation”, Journal of Mechanical Science and Technology, Vol 21, No 1, pg. 83-97.

Notation and List of Variables

a	Pressure dependent constant within the laminar leakage coefficient
a_0	Flow dependent coefficient
a_1	Displacement independent compressibility coefficient (Rydberg model)
a_2	Displacement dependent compressibility coefficient (Rydberg model)
a_3	Laminar flow coefficient (Rydberg model)
a_4	Analytical loss coefficient (best fit for axial piston pumps) (Rydberg model)
A_{piston}	Cross sectional area of a piston
b:	pressure and flow dependent constant within the laminar leakage coefficient
C_1, C_2, C_3, C_4, C_5	Loss coefficients (Zarotti and Nevegna model)
C_{C1}	Displacement independent compressibility coefficient (Olsson model)
C_{C2}	Displacement dependent compressibility coefficient (Olsson model)
C_{const}	Constant flow loss term
C_{CP}	Viscous flow coefficient (Pacey, Turquist and Clark model)
C_S	Laminar flow loss coefficient
C_S^*	Non-linear laminar flow loss coefficient (Dorey)
C_{ST}	Turbulent flow loss coefficient
C_{VN}	Valve plate notch loss coefficient (Jeong model)
C_{vPV}	Couette flow coefficient (Jeong model)
C_β	Bulk Modulus loss coefficient (Jeong model)
$C_{\mu PSV}$	Laminar flow loss coefficient (Jeong model)
d_{piston}	Diameter of a piston
f_{Pmax}	Displacement dependent polynomial fitted flow loss rate at maximum pressure (Huhtala model)
f_{Pmin}	Displacement dependent polynomial fitted flow loss rate at maximum pressure (Huhtala model)
f_v	Displacement setting dependent flow losses (Huhtala model)
$f_{\mu max}$	Pressure dependent polynomial fitted flow loss rate at maximum Viscosity (Huhtala model)
$f_{\mu min}$	Pressure dependent polynomial fitted flow loss rate at minimum Viscosity (Huhtala model)
H_{stroke}	Stroke height of the rotating group of an axial piston pump

k_{ijk}:	Loss coefficient (Ivantysyn and Ivantysynova model)
$K_{Q1} - K_{Q12}$:	Loss Coefficients (Kögl model)
n_{max}	Maximum operating speed of an axial piston pump
n_{min}	Minimum operating speed of an axial piston pump
n_{pump}	Pump input shaft speed
p_{atm}	Atmospheric Pressure
p_{case}	Pressure in the pump case
p_{hp}	Pressure on the pump outlet
p_{lp}	Pressure at the pump inlet
p_{max}	Maximum pressure in the measured data set (Huhtala model)
p_{min}	Minimum pressure in the measured data set (Huhtala model)
Δp_{sys}	Pressure rise from the pump inlet to outlet
$\Delta q_{V2,e}$	Average change in flow (from ISO 8426)
$q_1 - q_4$:	Loss Coefficients: (Ortwig)
Q_L	Total Flow Loss
Q_{L_COMP}	Compressibility flow loss coefficient (Bavendiek)
$Q_{L1} - Q_{L8}$	Flow loss coefficients (Bavendiek)
Q_{Lo}	Constant flow loss (Jeong model)
$q_{n,max}$	Pressure dependent polynomial fitted flow loss rate at maximum Pressure (Huhtala model)
$q_{n,min}$	Pressure dependent polynomial fitted flow loss rate at minimum Pressure (Huhtala model)
Q_{Pmax}	Speed dependent polynomial fitted flow loss rate at maximum pressure (Huhtala model)
Q_{Pmin}	Speed dependent polynomial fitted flow loss rate at minimum pressure(Huhtala model)
$Q_{v_{n,p}}$	Pressure and speed dependent flow loss (Huhtala model)
R_{piston}	Piston pitch radius in an axial piston pump
V_{max}	Maximum displacement of an axial piston pump
V_p	Ideal pump displacement
V_R	Ratio between the dead volume of the axial piston rotating group and displacement
z	Number of pistons in a pump
α	Swash angle of an axial piston pump
β_{fit}	Bulk modulus at fitting point (Huhtala model)
β_{oil}	Bulk modulus of the fluid
ε_p	Coefficient of displacement
μ:	Hydraulic fluid viscosity
μ_{max}	Maximum viscosity in the measured data set (Huhtala model)
μ_{min}	Minimum viscosity in the measured data set (Huhtala model)

$\boldsymbol{\rho}$: Hydraulic fluid density

CHAPTER 3. CALIBRATION AND CROSS-VALIDATION OF FLOW LOSS MODELS OF A HYDROSTATIC PUMP

A paper to be submitted to the *American Society of Mechanical Engineers*

Samuel J. Hall, Brian L. Steward

Abstract

Environmental legislation and rising fuel prices have increased the attention dedicated to increasing efficiency by designers of off highway vehicles and their components. This paper discusses a methodology for comparing flow loss models of closed circuit axial piston pumps, which are common on off-highway vehicle propulsion systems. Having the best mathematical representation of the flow losses in the pump will aid the designer in understanding the impact of flow losses on overall vehicle efficiency. The methodology consists of four steps to compare the flow loss models including: 1) calibration of complete models, 2) model term reduction through stepwise regression, 3) model term reduction by reducing multicollinearity, and 4) a leave one out cross validation (LOOCV). The Ivantysyn and Ivantysynova model clearly has the best performance in explaining the variability in the flow loss data set. However, in performing the LOOCV, there does not appear to be a significant difference between the Zarotti and Nevegna, Ivantysyn and Ivantysynova and the Jeong models in their performance to estimate the measured flow loss based on measured system variables not used for model calibration

Keywords: hydrostatic pump, linear regression, stepwise regression, leave one out cross validation, multicollinearity

3.1 Introduction

Legislation in the United States has dictated that the emissions of off-highway vehicles utilizing diesel engines must be reduced. New pollution controls will reduce the amount of NO_x and particulates emitted from diesel engines. The EPA has estimated that by the year 2030 these reductions will prevent 12,000 premature deaths, save 8,900 hospitalizations and one million lost work days annually [1].

As a result of these regulations, off-highway machine designers will be challenged by increased costs and space claim for engines. To this end, a large manufacturer of off-highway vehicles has stated that prices of their vehicles will rise by 12% on average due to equipment needed to comply with these regulations [2].

Hydraulic systems are common on these machines for power transmission and understanding the losses within the components is critical. A study from the United States Department of energy has estimated that the average hydraulic system is only 22% efficient. It is estimated that nearly a third of the inefficiency can be directly attributed to the components within the system, and the remainder attributed to the architecture of the hydraulic system [3]. This inefficiency further increases the need for accurate mathematical loss models of machine components during the design process.

One component that is common in industry is an axial piston pump that provides hydraulic fluid flow to the system. Not all of the flow that is swept by the rotating group is delivered to the outlet, the difference between the two is referred to as flow loss. Understanding and mathematically modeling the flow losses in these

pumps has been an area of study for over 60 years. The models of flow loss from the literature fall generally within one of three categories:

1) Physical flow loss models,
2) Numerical flow loss models, or
3) Analytical flow loss models.

Physical flow loss models characterize flow loss by utilizing loss terms that model physical interactions or processes within a pump. Common terms among these models are laminar, turbulent and compressible flows. Many of the models within this type use the Wilson model [4] and build on additional terms.

Numerical loss models characterize losses using terms that have little physical meaning, but have been shown to fit data sets well. Of these, the Ivantysyn and Ivantysynova model [5] is well recognized in the industry.

Analytical flow loss models use terms from both physical and numerical models to fit data. Table 3.1 is a list of notable loss models with the author, year they were published, and their model type [4] – [17].

The models developed in the literature all attempt to explain variation in the flow loss data, but with sets of model terms that vary in their composition and number. Some were constructed to only explain variability in measured data sets and others to attempt to quantify the amount of one type of loss or another. However, given the structure of some of the models, statistical problems may arise such as collinear terms or overfitting.

Table 3.1. Summary of the steady state loss models for hydraulic pumps including the number of variables within the models.

Author	Year	Model Type	Number of Terms
Wilson	1948	Physical	2
Schlösser	1961	Physical	2
Olsson	1973	Physical	4
Pacey, Turnquist and Clark	1979	Physical	2
Zarotti and Nevegna	1981	Analytical	5
Rydberg	1983	Analytical	5
Bavendiek	1987	Physical	11
Dorey	1988	Analytical	2
Ivantysyn, Ivantysynova	1993	Numerical	27*
Kögl	1995	Physical	11**
Huhtala	1997	Numerical	12
Baum	2001	Numerical	3 layers
Ortwig	2002	Numerical	3
Jeong	2006	Physical	6

* The Ivantysyn and Ivantysynova model can vary in the number of model terms based on the maximum exponent selected.
** Huhtala model coefficients based on test data at the extremes of the operating range, not based on the complete data set.

The work in this chapter investigates these issues with five selected flow loss models from the literature. The specific objectives of this study were to:

- Determine how well each of the full models can explain the variability in a measured flow loss data set.
- Determine if the models can be reduced by either stepwise cross validation or multicollinearity reduction without loss of performance
- Determine how well each of the full and reduced models generalizes the flow loss data set through cross validation.

3.2 Methods

Five of the above listed flow loss models were compared. The models were chosen to show the different types of models and see how each of them performs in estimating flow losses in a dataset from a 45 cm^3/rev closed circuit, axial piston pump (series H1, Danfoss Power Solutions. Ames, IA). The models included in this study were the three physical loss models from Wilson [4], Schlösser [6], and Jeong [17]; an analytical loss model from Zarotti and Nevegna [9], and the numerical model from Ivantysyn and Ivantysynova [5].

3.2.1. Overview of the Flow Loss Models

The Wilson flow loss model [4] is the earliest physical flow loss model, and many of the early flow loss models use this model as a starting point. The model consists of two loss terms: a laminar flow loss term and a constant flow loss term. The flow loss is represented mathematically as:

$$Q_L = C_S \frac{V_P \Delta p_{sys}}{2\pi\mu} + C_{constant} \tag{3.1}$$

The second flow loss model was developed by Schlösser [6]. Schlösser started with the laminar flow loss term from the Wilson model, but hypothesized that flow losses are better characterized using a turbulent loss term instead of a constant flow loss term. The flow loss is represented mathematically as:

$$Q_L = C_S \frac{V_P \Delta p_{sys}}{2\pi\mu} + C_{St} V_P^{\frac{2}{3}} \sqrt{\frac{2\Delta p_{sys}}{\rho}} \tag{3.2}$$

The Zarotti and Nevegna flow loss model [9] was developed principally to fit loss model data. Among the terms, the final two terms resemble a fluid

compressibility term and a power dependent term. The flow loss is represented mathematically as:

$$Q_L = C_1\Delta p_{sys} + C_2\Delta p_{sys}^2 + C_3\Delta p_{sys}^2 n_{pump}^{\frac{3}{2}} + C_4\Delta p_{sys} n_{pump} V_P + C_5\Delta p_{sys} n_{pump} \quad (3.3)$$

Ivantysyn and Ivantysynova [5] proposed a power model relating flow losses to pump displacement, input speed and the pressure increase across the pump. Additionally, Ivantysyn and Ivantysynova suggested that a viscosity-related set of terms could be added to span a range of operating temperatures. This set of viscosity dependent terms are added to the model for this study (p=q=r=2, s=1). The flow loss is represented mathematically as:

$$Q_L = \sum_{i=0}^{p}\sum_{j=0}^{q}\sum_{k=0}^{r}\sum_{\boldsymbol{l=0}}^{\boldsymbol{s}} k_{ijkl} V_p{}^i n^j \Delta p_{sys}{}^k \mu^l \quad (3.4)$$

Jeong [17] constructed a flow loss model based on the component interactions within a hydrostatic machine. Through inspection, many of the interfaces had terms that could not be mathematically differentiated from one another. These terms were then consolidated a reduced number of term included in the flow loss model. The terms are: 1) a laminar flow loss, 2) a Couette flow from sliding components 3) a turbulent loss term from the valve plate transition notches 4) A turbulent loss term due to rotating group filling, 5) a fluid compressibility term and 6) a constant leakage term. The flow loss is represented mathematically as:

$$Q_L = C_{\mu PSV}\frac{\Delta p_{sys}}{\mu} + C_{vPV} n_{pump} + C_{VN}\sqrt{\frac{\Delta p_{sys}}{\rho}} + C_{PP}\frac{\rho n^3}{\Delta p_{sys}} + C_\beta n_{pump}\Delta p_{sys} + Q_{Lo} \quad (3.5)$$

Within the flow loss models, system variables such as the pressure rise across the pump, Δp_{sys}, the input speed of the pump n_{pump} can be provided from measurements directly. However, in many of the models, the dynamic viscosity of the fluid, μ, is needed as well. In this work, a model for viscosity was used to estimate viscosity as a function of fluid temperature. This relationship is represented mathematically as:

$$\mu = (\rho_0 - \rho_T) * \eta_0 e^{-kT_{oil}} \tag{3.6}$$

where

$\rho_0$is the oil density at a reference condition
$\rho_T$is the rate of change of oil density with temperature
η_0, is the reference kinematic viscosity
k is the kinematic viscosity constant

The model coefficients were estimated from fluid product data (Shell Tellus ISO VG 46).

3.2.2 Statistics Background

To determine the coefficients within the flow loss models, a common method was used across all of the models. Since the coefficients were linearly related to the terms within the models, linear regression was a suitable method of determining the coefficients within the models. Specifically, ordinary least squares regression [20] is a common method that minimizes the sum of the squared error between the model and the measured data set.

The structure of a linear model is the measured data set y, is equal to the coefficient(s) that the regression will determine β, multiplied by the independent variables, X, plus the error ε.

$$y = X\beta + \varepsilon \tag{3.7}$$

The OLS regression method minimizes the sum of squared residuals to determine the value of the estimated model coefficient, $\hat{\beta}$:

$$\hat{\beta} = (X^T X)^{-1} X^T y \tag{3.8}$$

The metric for comparison of the models is the Root Mean Squared Error (RMSE). The RMSE was calculated by determining the square root of the sum of the difference between the modeled, $\hat{y}$, and measured values, y, of the independent variable divided by the total number of data points, n, shown as:

$$RMSE = \sqrt{\frac{\sum_{i=1}^{n} (\hat{y} - y)^2}{n}} \tag{3.9}$$

Stepwise linear regression uses the Bayesian information criterion to determine which components of the model best describe the data. This method is accomplished by progressively adding terms, calculating the criterion and determining if there is an optimum value of the BIC for a sub model [19]. The BIC is calculated with the maximized value of the likelihood function of the model, $\hat{L}$, the number of free terms in the model, k, and the number of data points, *n* written as:

$$BIC = -2\,\mathrm{LN}(\hat{L}) + k * \mathrm{LN}(n) \tag{3.10}$$

The BIC criterion decreases as the number of terms increases during stepwise regression (Figure 3.1). The example in figure 3.1 is the BIC from a stepwise regression procedure for the Ivantysyn and Ivantysynova model. Starting with zero terms, the BIC was calculated and recalculated as the number of model

terms increased. This process continued until the stopping condition of the method was reached at 25 of the 54 terms. The minimum value of the BIC occurred at 15 terms signified with the vertical line. This result is interpreted as the sub model that best represents the data with the minimum number of terms.

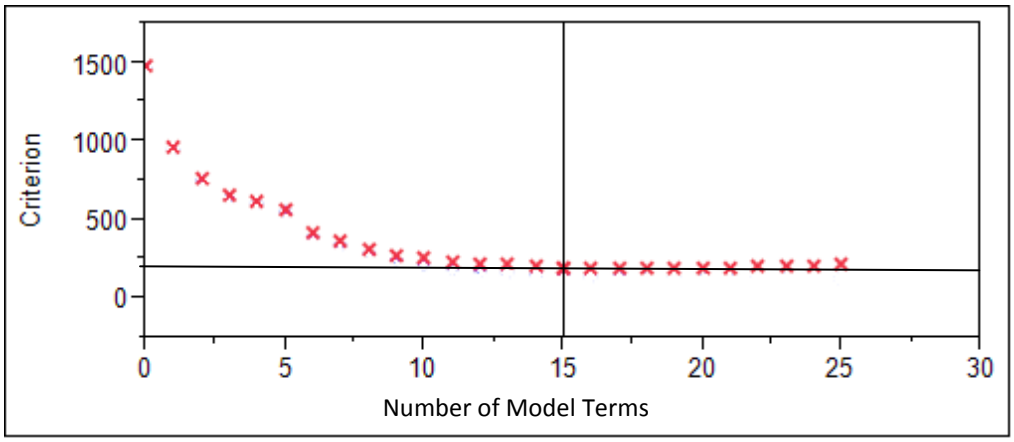

Figure 3.1. BIC criterion as a function of number of model terms during stepwise regression.

3.2.3 Experimental Methodology.

The methodology for comparing the performance steady-state flow loss models of hydraulic, axial piston pumps was a four-step process. First, the models were calibrated to determine how well each of the flow loss models explains the variability in the measured data. This calibration was accomplished by constructing a common pump flow model framework that into which all of the various flow models were placed. This framework provides a data set for which a linear regression obtained flow loss model terms.

The second step was to determine if the full pump loss model can be reduced and still explain the variability in the flow loss data set. This reduction was accomplished using stepwise regression and Bayesian Information Criterion (BIC).

This method determines the best trade-off between model complexity and goodness of fit. Additionally, over fitting is also reduced due to the most significant terms being added first.

The third step is a reduction of the flow loss models by removing multicollinearity within them. The method consists of examining model terms that are collinear with one another and then eliminating the term that is more likely to have a coefficient that is equal to zero. A comparison of the calibration error will also be included.

The fourth step will use leave one out cross validation (LOOCV) to compare the complete and reduced models. The LOOCV of both the complete models and the reduced models will give insight to if both models were over-fitting the data and how well each of the models characterizes the pump losses.

3.2.4 Flow Loss Determination from Measured Data

The basis for calibrating a flow loss model is accurate flow data. The data used for this study was collected based on the standard pump test found in the international standard for testing steady state performance of pumps and motors, ISO4409 [20] . All of the instruments were in accordance with accuracy class “A” of the ISO standard. Data for the test was acquired from an 45 cm^3/rev closed-circuit axial piston pump test (Series H1, Danfoss, Ames, IA; Figure 3.2).

Flow loss measurements were acquired across the variation of four experimental factors with corresponding numbers of levels. These factors and levels included two temperatures, four displacement settings, five input shaft speeds and six differential pressures resulting in a dataset with a possible two hundred and forty

data points (Table 3.2). However, four flow loss measurements could not be collected at both temperatures, the slowest shaft speed, and the lowest displacement with the two highest pressures, reducing the data set to flow loss measurements at 236 combinations of experimental factors.

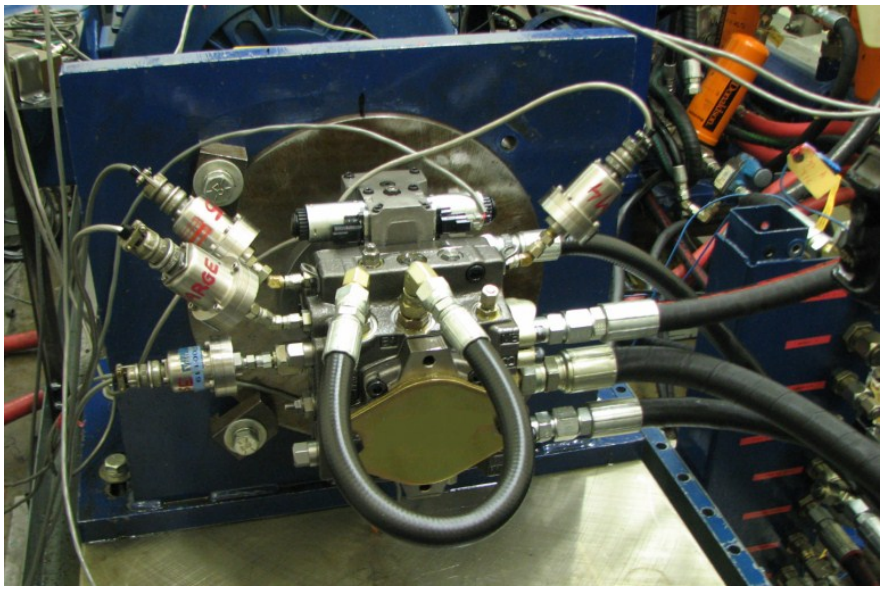

Figure 3.2. A 45 cm^3/rev closed circuit, axial piston pump during testing.

Table 3.2. Pump test stand levels of experimental treatments to generate the loss data set.

Pressure (Pa)	Speed (Rad/s)	Displacement (%)	Temperature (˚C)
1e6	52.4	20	50
5e6	104.7	40	80
1e7	209.4	80	
2e7	314.2	100	
3e7	366.5		
4e7			

In the test circuit, a mixture of charge flow and return flow, Q_{inlet}, enters the pump inlet (Figure 3.3). The flow then enters the rotating group, cross-port flow losses, $Q_{L,int}$, leak back to the inlet, and case drain flow losses, $Q_{L,ext}$, flow out to the

pump case. The flow from the pump output, Q_{outlet}, flows through the relief valve before being measured, filtered, cooled and then recirculated to the inlet.

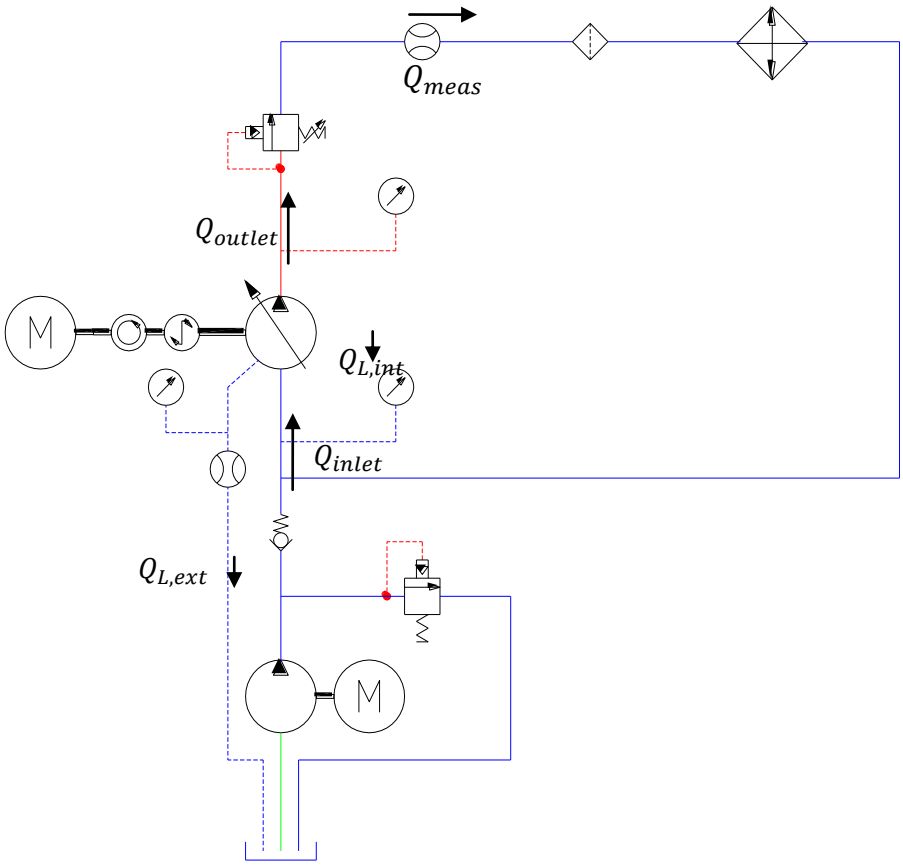

Figure 3.3. Schematic of the pump flow test rig for which the flow loss data is taken from.

To determine the pump flow loss, both the ideal flow, and the flow out of the pump outlet must be known. The flow out of the outlet can be determined based on the flow measured downstream of the relief valve and the effective flow loss due to compressibility of the hydraulic fluid, $Q_{B.mod}$ in the test rig [5] and is shown as:

$$Q_{outlet} = Q_{meas} - Q_{B.mod} \tag{3.11}$$

where

$$Q_{B.mod} = n * V_P * \frac{\Delta p_{sys}}{\beta_p \Delta p_{sys} + \beta_T T_{oil} + \beta_0} \tag{3.12}$$

β_p is the isothermal compressibility coefficient of fluid,

β_T is the volumetric expansion coefficient of fluid,
β_0 is the reference bulk modulus of the fluid.
Δp_{sys} is the pressure rise from the pump inlet to the pump outlet

The bulk modulus flow term is used to describe how the volumetric flow rate changes across the relief valve, and yet the mass flow rate coming into and going out of the relief valve are equal.

The total flow loss out of the pump, Q_L, is the sum of the internal flow loss, $Q_{L,int}$, and the external flow loss, $Q_{L,ext}$ and the compressibility flow. It is also equal to is defined then as the difference between the ideal flow out of the pump and the flow out of the pump outlet mathematically shown as:

$$Q_L = Q_{L,ext} + Q_{L,int} + Q_{B.mod} = Q_{ideal} - Q_{outlet} \tag{3.13}$$

The ideal flow is defined as the product of ideal displacement multiplied by the measured input speed. The ideal displacement for this study was calculated using the Toet method [21], using data points at an array of speeds and pressures with the pump servo piston mechanically locked in place.

The Toet method for calculating ideal pump displacement utilizes a similar method of multiple interpolations, but reverses the order to determine the ideal displacement. The first step of Toet's method is to regress the flow rate onto shaft speed for each of different test pressure difference across the pump outlet and inlet and the test temperature. The slope of each of these regression lines from the first step are then regressed against the measured pressure difference across the pump (Fig. 3.4). The ideal displacement is set to be the y-intercept of the regression line from the second step.

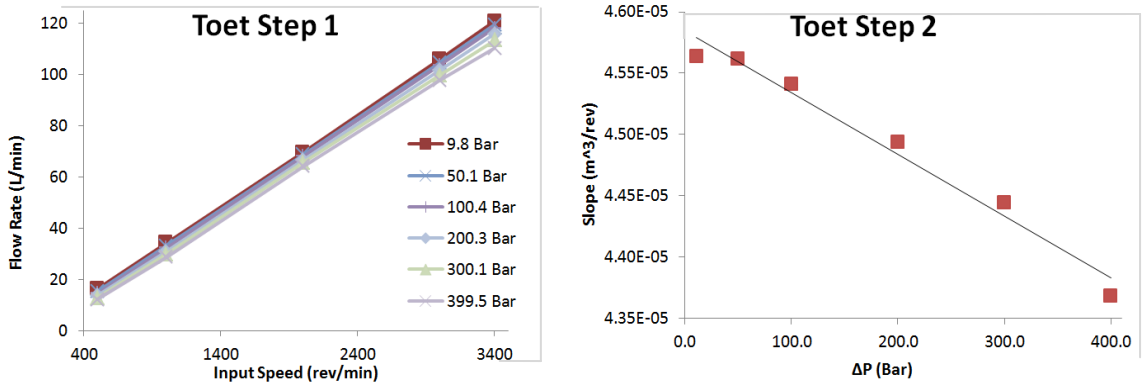

Figure 3.4. Graphical depiction of the Toet method for calculating Ideal displacement.

3.2.5 Calibration of Flow Loss Models using Linear Regression

The comparison of loss models starts with the calibration of a model to the measured data set. For this study, each of the models was calibrated to the complete data set. Then, the models were compared based on their performance in explaining the variability in the loss data. The performance metric used was the Root Mean Squared Error (RMSE) of each of the models with the given data set.

All five of the models have non-linear terms with respect to the system parameters of the pump under test. However, the models either were already or were mathematically manipulated so that they were linear in their coefficients. This approach enabled the use of ordinary least squares (OLS) linear regression [18], as a valid method of determining coefficients for a given model. The regression was performed using the “Fit Model” functionality with the commercial statistical package JMP Pro® (JMP Pro V10, Statistical Analysis System Institute; Cary, North Carolina).

3.2.6 Stepwise Regression

The second portion of the model comparison was to examine the models and determine if they over-fit the data. Stepwise regression analysis was employed to determine the set of model terms that described the most variation with the minimum number of terms. Stepwise regression was carried out using forward selection and the Bayesian Information Criterion (BIC). JMP Pro® was also used for this task.

3.2.7 Reduction of Flow Loss Models due to Multicollinearity

An issue that can arise in statistical modeling is that two or more model terms can be linearly related. This correlation between terms can have a detrimental effect on model performance. Strong interactions between model terms that can have significant influence on model coefficient values with very little numerical difference between input data. These issues are commonly referred to in literature as multicollinearity [18].

An assumption that is made when performing OLS linear regression is that none of the model terms within the model are “perfectly collinear”; meaning that there is not an exact linear relationship between model terms. If perfectly collinear pairs do exist, the rank of the variable matrix X (from equation 3.9) will be less than the number of observations plus one, and the matrix will not be invertible. This singularity will cause the least squares calculation to fail.

Perfect collinearity is uncommon in measured data; however, mathematical models can have terms that are mathematically identical, but may be based on understood sources. An example of this can be found in the unreduced Jeong flow loss model. The laminar flow loss terms representing the laminar flow between the

slippers and the swash plate and the laminar flow between the cylinder-block and valve-plate are both represented by the pressure increase across the rotating group Δp_{sys}, divided by the fluid viscosity μ multiplied by the coefficient. The final version of the Jeong flow loss model combines these model terms, and the model does not attempt to distinguish between the two sources.

High multicollinearity is more prevalent in statistical modeling and is characterized by highly-correlated model variables [22]. In this case, even though the X^TX matrix from equation 3.8 is invertible, the matrix will be ill-conditioned and thus can have numerical problems, such as small differences in the data set leading to large differences in model coefficient values and model coefficient confidence intervals.

Multicollinearity can be detected by a number of different methods. The following are common methods of detecting multicollinearity: 1) the p-value of F-test rejecting the null hypothesis that all of the model coefficients are zero for the complete model is low, but few to none of the individuals coefficients have a low p-value from the associated t-test, 2) a variance inflation factor (VIF) of >10 of model coefficients, and 3) the correlation coefficient between two model terms is greater than a set value (0.8 to 0.9 are typical) [23].

3.2.7.1 P-Value Examination to Determine Multicollinearity

The first method of examining for multicollinearity uses the p-value for the model F-test and that of the t-test for the individual model terms to determine if multicollinearity may be present. The p-value is the probability that the null hypothesis for a linear model is incorrect; the null hypothesis is that all of the model

coefficients are equal to zero. Another way of stating it is the probability that at least one of the model terms explains some variability in the dependent data set.

In the case of models that have independent variables that have high levels of collinearity, the p value for the complete model is low, and many of the model coefficient p-values are high. This should be interpreted to mean that the complete model has model coefficients that are non-zero, but each of the model coefficients cannot be determined to be non-zero. This suggests that the model term either is not significant or can be compensated with by another model term.

3.2.7.2 Multicollinearity Determination using VIF

The variance inflation factor (VIF) is an aid in quantifying the amount of multicollinearity that may be present in a linear model. The VIF of a regression coefficient measures how much the variance of that term has been increased due to collinearity with any and all of the other coefficients within the model.

The VIF of a model term can be expressed as the inverse of the one minus the square of the standard error of R_j^2, of all of the other independent terms in the model when linearly regressed to a given term (Eq. 3.14); The goal being to determine if the model term is correlated with the remaining terms in the full model.

$$VIF = \frac{1}{\left(1 - R_j^2\right)} \tag{3.14}$$

That is, the VIF indicates how well can a linear model be constructed of every model term less the one model term that was left out. A down side of the VIF is that it is a scalar value and only indicates that multicollinearity is present. The VIF does not direct one to the set of other model terms to which a particular term may be

collinear. Thresholds of VIF that indicate if multicollinearity may be present vary in the literature between 5 [18] and 10 [22].

3.2.7.3 Multicollinearity Determination using Model Term Correlation Coefficients

For linear model terms that exhibit high levels of collinearity, one method of improving the model is to reduce the number of model coefficients. This method consist of two steps: 1) determining variable pairs that are highly linearly correlated and 2) removing one of each pair of correlated variables. This methodology will remove model term pairs that are highly correlated and reduce the possibility of over fitting the data set.

To determine the pairs of variables that are highly linearly correlated, the correlation coefficients between each of the variables is calculated for all possible model term pairs [24]. The Pearson correlation coefficient is a measure of linear correlation between two model terms in a model. An example of this is shown in Table 3.2 which is taken from the Zarotti and Nevegna model discussed later. Since the matrix is symmetric by nature, so only one half of the correlation matrix is needed and the other half is blacked out. Additionally, the 1:1 relationship between a model term is blacked out to only consider the model term inter-relationships.

Table 3.3. Pearson correlation matrix of independent variables in the full Zarotti and Nevegna model.

	C_1	C_2	C_3	C_{45}	C_5
C_1					
C_2	0.9668				
C_3	0.7138	0.7403			
C_{45}	0.7618	0.7401	0.9647		
C_5	0.5106	0.4978	0.7968	0.8111	

Many statistical software packages also display a scatter plot matrix of the correlation matrix as is shown in Figure 3.5. The red lines are the bivariate normal density ellipse of a given percentage. That is, 95% of the data points are within the ellipse. This aids in visualizing the relationships between variables. For instance, C_1 and C_2 have a correlation coefficient of 0.9668 and appear to highly linearly correlated while C_1 and C_5 are not and have a high correlation coefficient of 0.5106.

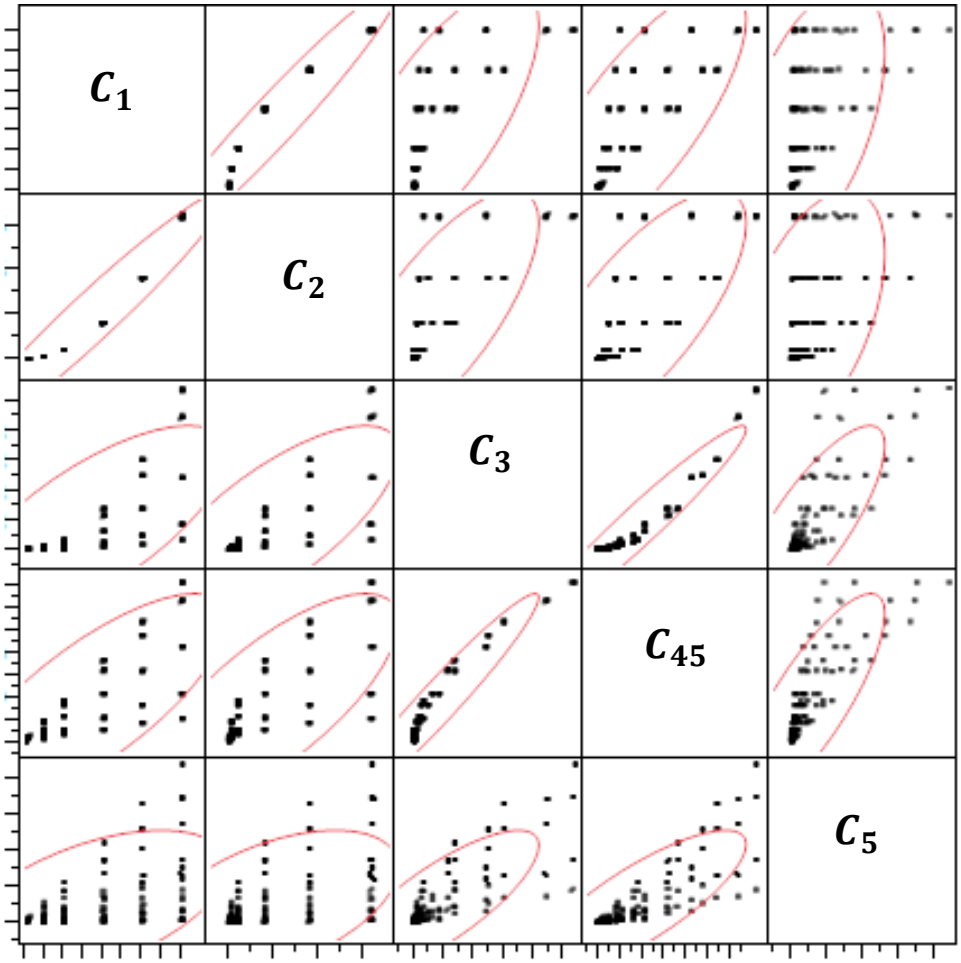

Figure 3.5. Example of a scatter-plot matrix array for all of the model terms within the complete Zarotti and Nevegna flow loss model.

Once the correlation coefficients are determined, and if the correlation coefficients are large enough, the model should be reduced. To systematically

approach this task, all of the correlation coefficients above a threshold should be listed and model coefficient that has the largest p-value from the initial calibration should be dropped. That is, the variable of the two that is most likely to be equal to zero of the two model terms should be dropped. The threshold of the correlation coefficient should be between 0.8 and 0.9 [23].

3.2.8 K-Fold Cross Validation

Cross-validation is a statistical method of determining how well a model characterizes a data set that is independent of the calibration data set. This method can help to determine which of multiple models may have the best predictive performance. Cross-validation may also aid in determining if a particular model is over-fitting a data set.

In academia and industry, resources are limited, limiting the amount of data available to a researcher or engineer. This limited amount of data drives one to use a model cross validation methods. The k-fold cross validation, uses a single data set, but divides it up the complete data set into groups called folds. These folds are then divided into a teaching data set to which the model is calibrated to and the validation data set to which the model output is compared. This process is repeated for all of the folds, and the root mean squared error (RMSE) between the model output and the measured output is calculated.

An illustration of k-fold cross validation is illustrated in table 3.4. The Method would start by calibrating a model to k-folds 2 through 4 and then calculate the errors of estimation the data in k-fold 1. The process is then repeated for all four folds and the RMSE of each of the points is then calculated.

Table 3.4: Illustration of a k-fold cross validation.

K-Fold 1			K-Fold 2			K-Fold 3			K-Fold 4		
Data 1	Data 2	Data 3	Data 4	Data 5	Data 6	Data 7	Data 8	Data 9	Data 10	Data 11	Data 12

The guidance on the number of folds varies among authors with typical guidance being 10 [25] or equal to the number of samples. The method that uses the same number of folds as number of observations is commonly referred to as leave-one-out cross validation (LOOCV). LOOCV is computationally the most expensive since the number of regressions is equal to the number of observations, but the training data set for each model calibration is as large as possible. LOOCV was used in this study because of the relatively small perceived difference in the computation time between either a small number of folds or a complete LOOCV.

3.2.9 Analysis

The data set for the study was collected during qualification testing of a 45 cm^3/rev closed circuit axial piston pump (series H1, Danfoss, Ames, Iowa). The test conditions are the set of all possible combinations of pressure, speed, pump displacement and oil temperature shown in Table 3.2. This experimental design yielded 240 conditions. This array of data was selected based on the criteria specified in ISO 4409 [20].

To keep with the intent of ISO 4409, and given that the test rig was set up with the location of the flow meter being in the alternate location, after the relief valve (Fig. 3.3), the flow at the outlet of the pump must be calculated based on the measured flow and the known bulk modulus. Additionally, the ideal or theoretical pump displacements were determined using Toet's Method. A commercially

available statistical software package (JMP Version 10, SAS Institue, Cary, North Carolina) was used to perform the linear regression for both steps of Toet's Method. This same software is used for all of the regression in this work less the cross validation.

The ideal pump flow rate was determined given the measured input speed for each test run and the derived ideal displacement. The pump flow loss was subsequently determined as the difference between the ideal flow and effective pump outlet flow. These calculations were performed in an Excel spreadsheet (Microsoft Excel 2010, Microsoft Corporation, Redmond, Washington). With the flow loss tabulated, the flow loss models were calibrated; cross validated and compared using this data set.

3.2.9.1 Calibration of Complete Models

The first step of comparing the models started with an initial calibration of each of the five flow loss models. The models will initially be compared by using the root mean squared error (RMSE) statistic. This statistic shows how well each of the models can explain the variability in the flow loss data.

In addition, an initial assessment determined if multicollinearity may be an issue with the model. First, the p-value of the complete model was compared with the p-value of the model coefficients. If the model p-value indicates that the model has one non-zero model coefficient and very few to none of the model coefficients were likely to be equal to zero, multicollinearity may be an issue.

The second indicator of possible multicollinearity was the VIF. The VIF is a statistic that shows how much the confidence interval for a given model coefficient

within the linear model is increased due to linear correlations with other model terms. A VIF that is greater than ten indicated that a model term is heavily correlated with another and may need to be removed to prevent over-fitting [18]. Both of these sets of statistics were calculated when performing a linear regression.

3.2.9.2 Model Reduction through Stepwise Regression

The first method used to reduce the number of terms within the model and the possibility of over-fitting was stepwise regression analysis. The stepwise regression algorithm for this work was step-forward along with BIC criteria. This method added model terms in the order of those which explained the most variation in the data until there is a relative minimum in the calculated BIC of the reduced model (Figure 3.4). The stepwise regression was performed using JMP Pro 10 in the “Fit Model” utility. The intent of model reduction was to explain as much of the variability of a data set with the minimum number of model terms from a given model.

3.2.9.3 Model Reduction through Collinearity Analysis

The second method for model reduction excluded model terms that exhibit high levels of multicollinearity. This exclusion was accomplished using a two-step process. The first step generated a correlation matrix between all of the model terms within the model. The correlation matrix gave an indication of how linearly related were all pairs of model terms. The elements of the correlation matrix varied from zero to positive or negative one [18].

Secondly, the model was reduced by examining the correlation coefficient matrix to see which combinations of terms had a correlation coefficient larger than a threshold value. The model term that would be removed is the term with the larger

p-value from the full model calibration. The threshold value of the correlation coefficient for this study was 0.85; the mean of the recommended range of 0.8 and 0.9 [23]. The reduced models were calibrated to determine if there was a significant reduction on the RMSE.

3.2.9.4 Leave One Out Cross Validation of Complete and Reduced Models

The final point of comparison of the models was a complete leave one out cross validation. Three versions of each of the models were evaluated: 1) the complete model, 2) the stepwise regression reduced models and 3) the multicollinearity analysis reduced models. The models were compared across the different models and the versions each models. The leave one out cross validation (LOOCV) [24] was carried out using scripting and the statistical toolbox in MATLAB (version 2013b, MathWorks, Natick, Massachusetts).

The RMSE of cross validation was compared across of all three versions of each model. RMSE of cross validation gave an indication to how well a model may predict a data set and an indication if the model was over-fitting the data set. The prediction comparison helps one to infer how well each of the models will predict an independent data set. The second inference was made by comparing the RMSE of LOOCV and the model calibration. If the RMSE of LOOCV is significantly higher than that of the original calibration, this is in indicator that the model overfit the calibration data set and may not generally characterize the pump flow loss behavior.

3.3 Results and Discussion

3.3.1 Calibration of Complete Models

The calibration of all five flow loss models vs. the measured flow loss data is summarized in figures 3.6, 3.8 and 3.10 through 3.12. The cross plot displays the measured flow losses on the x-axis and the modeled loss on the y-axis. Also included is a solid 1:1 line that if the model were to equal the data, the point would be directly on the line. All of the losses are in liters per minute (L/min) of flow loss.

The cross plot for the Wilson model (Fig. 3.6) shows a poor correlation between the measured and modeled flow loss with much scatter about the 1:1 line. The Wilson model constant was slightly more than 3.9 L/min thus resulting in the no predicted flow losses less than 3.9 L/min. Additionally, pump shaft speed was not taken into account in this model.

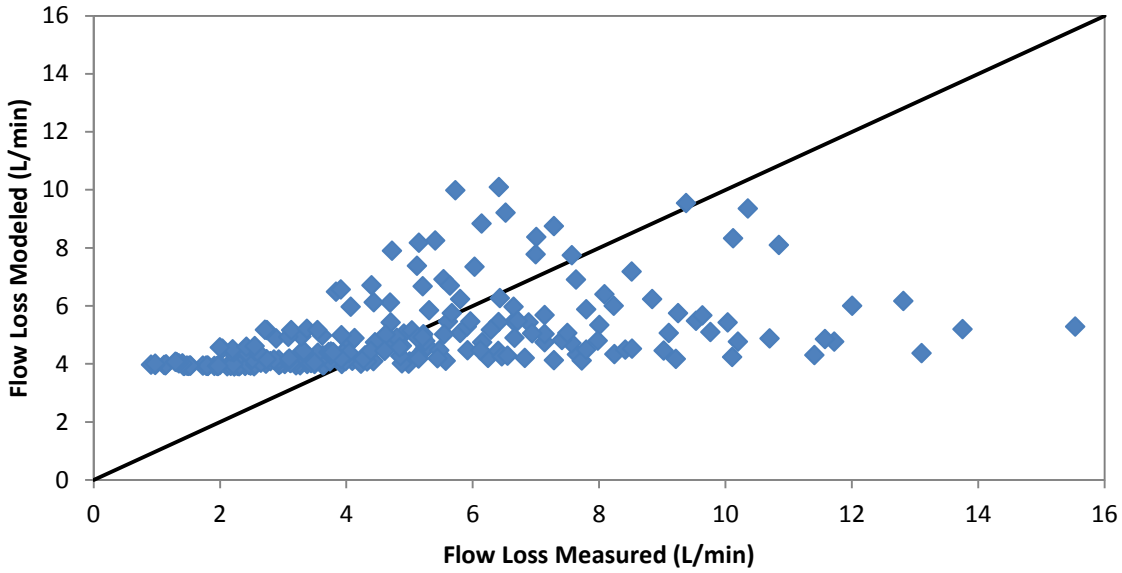

Figure 3.6. Cross plot of measured vs. modeled flow loss for the complete Wilson flow loss model.

Examining the model from another perspective, the measured flow loss was regressed onto the laminar flow loss term (Fig. 3.7) plus a constant. At low values of the laminar term, the measure flow loss data point were scattered both below and above the regression line. The R^2 of 0.211 between the laminar term and the measured flow loss suggests that laminar flow loss was not sufficient by itself to model flow losses for these data.

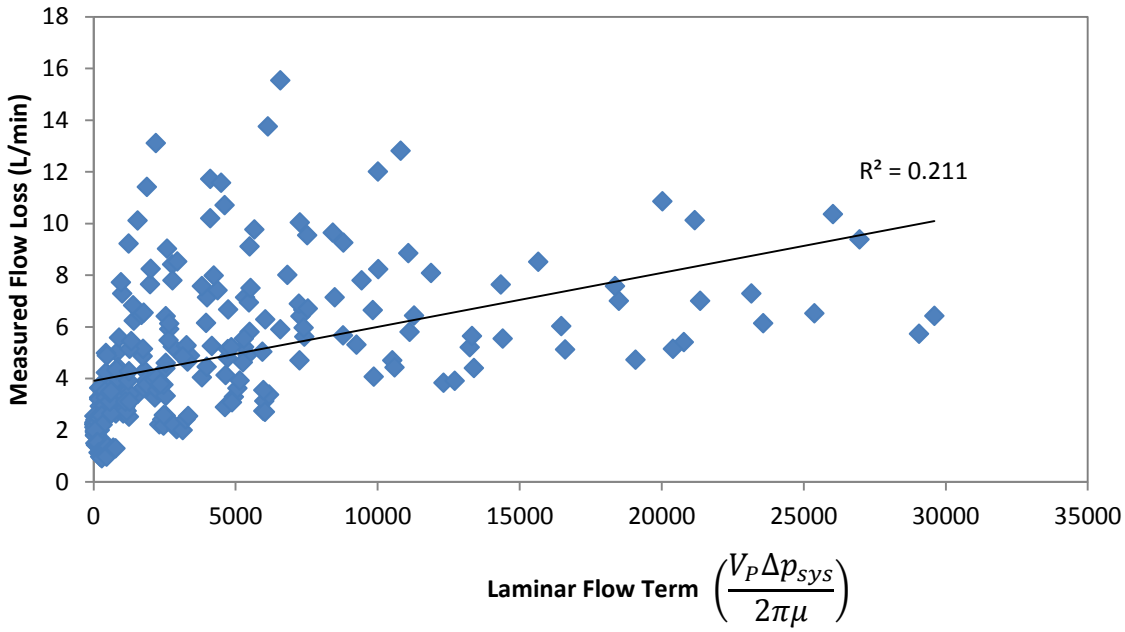

Figure 3.7. The relationship between the laminar flow loss term and the modeled flow loss in the full Wilson flow loss model.

The Wilson model has a model p-value of less than 0.0001 as does both of the model coefficients. The two model coefficients within the model both have a VIF less than ten. This leads one to believe that multicollinearity was not an issue with the model. This intuitively makes sense because the first term was dependent on displacement, pressure and fluid viscosity while the second term was a constant.

Table 3.5. Model coefficient p-values and variance inflation factors of the full Wilson model.

Model p-value		<.0001*	
Term	**Coeff. value**	**Coeff. p-value**	**VIF**
C_S	2.089e-4	<.0001*	1.6
$C_{constant}$	3.904	<.0001*	1.6

The Schlösser model (Figure 3.8) has an increasing scatter in the modeled flow loss as the measured flow loss increases. Since the Schlösser model does not have a constant term, the flow loss intercept is forced to be zero, and so the model could be improved with the addition of a constant term. The model has a RMSE 2.814 L/min; the largest of the full flow loss models.

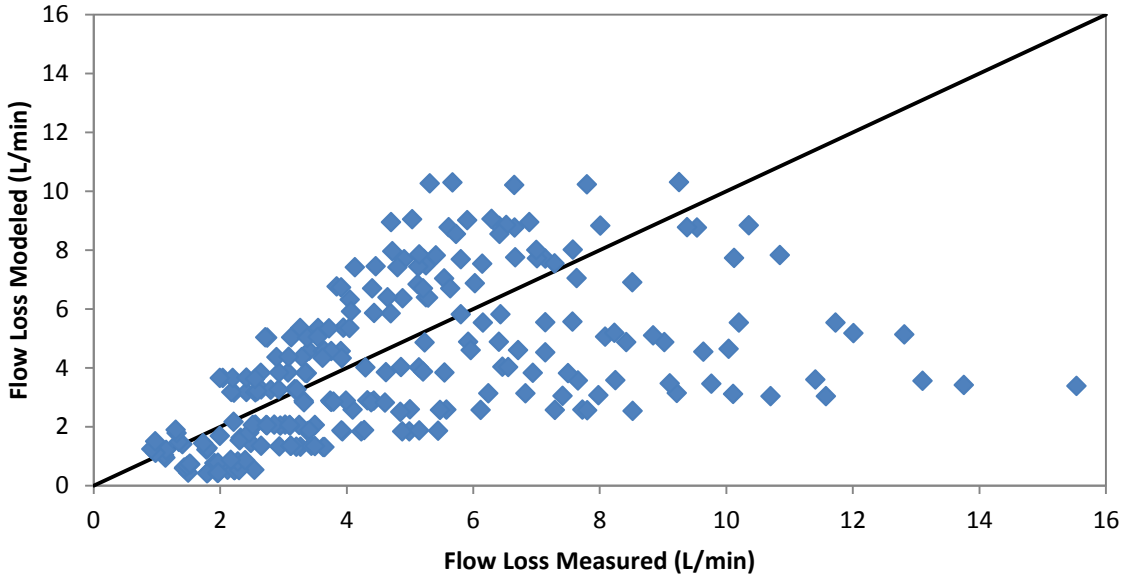

Figure 3.8. Cross plot of measured vs. modeled flow loss, post calibration for the full Schlösser flow loss model.

To examine the lack of fit associate with the Schlösser model, the turbulent term (Fig. 3.9) was investigated in a similar manner as the laminar term of the Wilson model. There was an R^2 0f 0.2946 between the turbulent term and the measured flow loss. Many of the test conditions with the largest flow loss have the

largest deviation off the regression line. Many of these data points were at low displacements, larger shaft speeds, and higher delta pressures. From these results, it appears that additional model terms must be added to the model to better explain variability in the flow loss data.

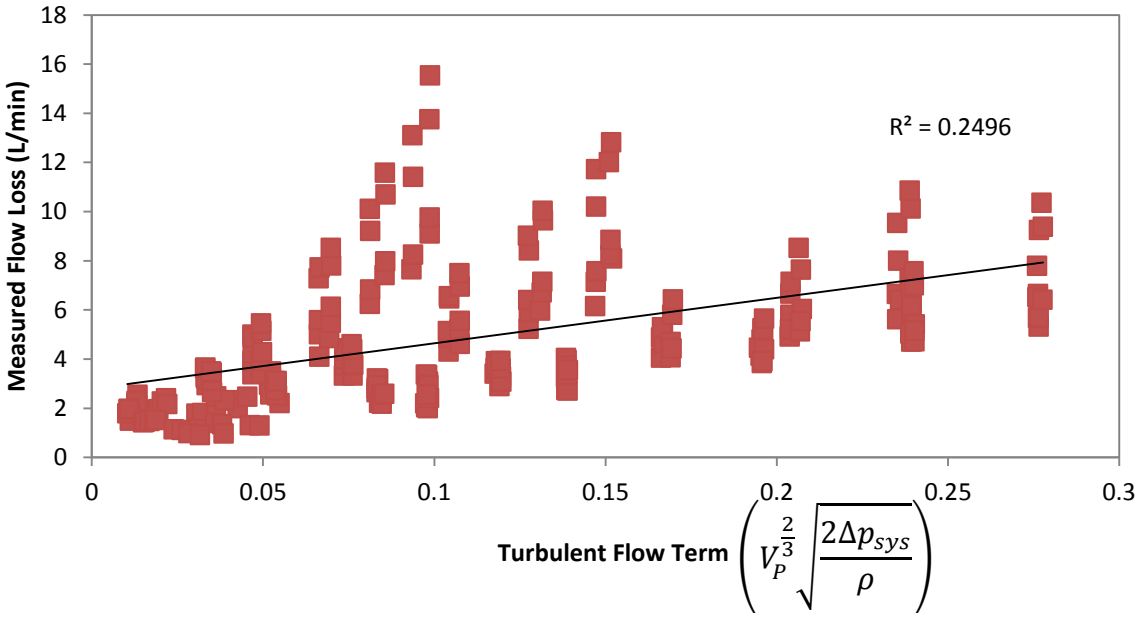

Figure 3.9. Cross plot of the turbulent flow loss term to the full Schlösser flow loss model.

The Schlösser model had a p-value of less than 0.0001 as did as the turbulent loss term, C_{ST}, (Table 3.6). However, the coefficient associated with the laminar flow loss term, C_S, had a very small magnitude and was not significantly different than zero. The two model terms both have a VIF less than ten, which indicated that multicollinearity was not an issue with the model.

Table 3.6. Model coefficient p-values and variance inflation factor of the full Schlösser model.

Model p-value		<.0001*	
Term	**Coeff. Value**	**Coeff. p-value**	**VIF**
C_S	-8.666e-5	0.0676	3.9
C_{ST}	40.006	<.0001*	3.9

The Zarotti and Nevegna model exhibited substantially better performance than the two physical process based flow loss models with a RMSE of 1.083 L/min (Fig 3.10). There appears to be slight non-linear characteristic to the modeled vs. measured relationship; an additional term may help to address this. The addition of a constant term may be able to help as well.

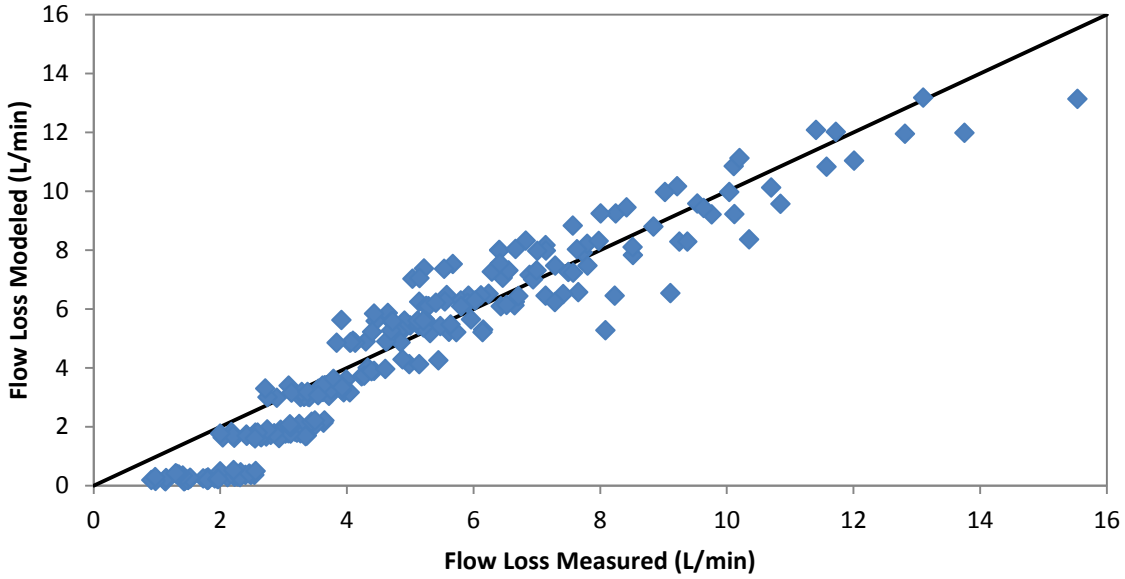

Figure 3.10. Cross plot of measured vs. modeled flow loss, post calibration for the full Zarotti and Nevegna flow loss model.

The Zarotti and Nevegna model has p-value of less than 0.0001 and each of the five model coefficients were statistically significant (Table 3.7). However, examining the VIF of the model coefficients, four of the five coefficients have a value of greater than ten. This indicates that some of the model terms have linear

dependencies with one another. It may be possible that a reduced model could have similar predictive capability, but multicollinearity could be reduced.

Table 3.7. Model coefficient p-values and variance inflation factor of the full Zarotti and Nevegna model.

Model p-value		<.0001*	
Term	**Coeff. value**	**Coeff. p-value**	**VIF**
C_1	3.360E-07	<.0001*	58.3
C_2	-8.79E-15	<.0001*	40.7
C_3	3.862E-19	0.0059*	40.1
C_{4_5}	4.292E-10	<.0001*	61.7
C_5	-2.78E-12	<.0001*	4.5

The Ivantysyn and Ivantysynova model explained most the variability in the flow loss data with most of the data points lying on or close to the 1:1 line (Fig 3.11). This model had the lowest RMSE of calibration of all the full models at 0.304 L/min. The primary point of concern for the model was the large number of model terms, 54, and the possibility of multicollinearity with only 236 measured data points.

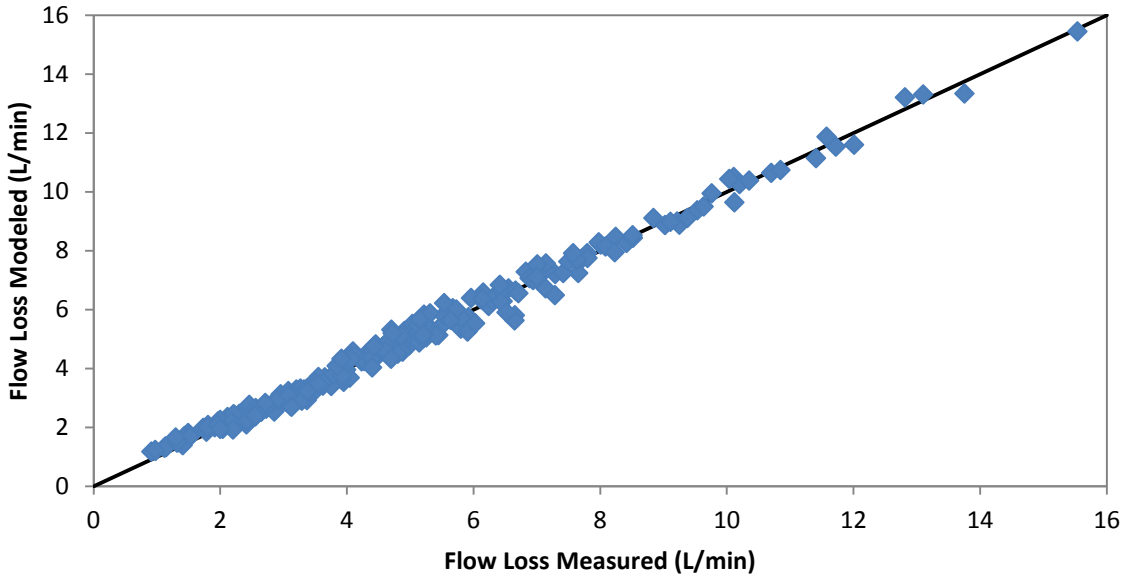

Figure 3.11. Cross plot of measured vs. modeled flow loss, post calibration for the full Ivantysyn and Ivantysynova flow loss model.

The Ivantysyn and Ivantysynova flow loss model has a p-value of less than 0.0001 (Table 3.8). However, of the fifty four model coefficients, none of them were statistically different from zero, leading to the conclusion that there was a high level of multicollinearity inside the model. Additionally, the VIF values for each of the model coefficients was extremely high varying from just over eight thousand to over six million. This finding was not unexpected due to the model being a power model of four system parameters. Even though this model explains most of the variability in the flow loss data, it was apparent that the model should be reduced to remove multicollinearity and at the same time determine if the reduced model can yield similar performance.

Table 3.8. Model coefficient p-values and variance inflation factor of the full Ivantysyn and Ivantysynova model.

Model p-value		<.0001*	
Term	**Coeff. value**	**Coeff. p-value**	**VIF**
I_{01} $(\Delta p^0 n^0 \alpha^0 \mu^0)$	1.321E+00	0.503	9723.4
I_{02} $(\Delta p^0 n^0 \alpha^1 \mu^0)$	1.525E+00	0.952	75862.9
I_{03} $(\Delta p^0 n^0 \alpha^2 \mu^0)$	-6.683E+00	0.917	39139.0
I_{04} $(\Delta p^0 n^1 \alpha^0 \mu^0)$	4.354E-03	0.860	88167.2
I_{05} $(\Delta p^0 n^1 \alpha^1 \mu^0)$	-2.958E-02	0.925	674664.0
I_{06} $(\Delta p^0 n^1 \alpha^2 \mu^0)$	-4.084E-02	0.960	347085.2
I_{07} $(\Delta p^0 n^2 \alpha^0 \mu^0)$	-1.170E-06	0.984	50611.3
I_{08} $(\Delta p^0 n^2 \alpha^1 \mu^0)$	-6.000E-05	0.937	386503.3
I_{09} $(\Delta p^0 n^2 \alpha^2 \mu^0)$	4.451E-04	0.818	198702.5
I_{10} $(\Delta p^1 n^0 \alpha^0 \mu^0)$	6.882E-08	0.802	92293.8
I_{11} $(\Delta p^1 n^0 \alpha^1 \mu^0)$	1.028E-06	0.764	709544.6
I_{12} $(\Delta p^1 n^0 \alpha^2 \mu^0)$	-2.231E-06	0.798	362116.1
I_{13} $(\Delta p^1 n^1 \alpha^0 \mu^0)$	1.591E-09	0.634	810040.5
I_{14} $(\Delta p^1 n^1 \alpha^1 \mu^0)$	-1.558E-08	0.711	6092449.4
I_{15} $(\Delta p^1 n^1 \alpha^2 \mu^0)$	3.520E-08	0.742	3112848.6
I_{16} $(\Delta p^1 n^2 \alpha^0 \mu^0)$	-2.930E-12	0.713	454656.1
I_{17} $(\Delta p^1 n^2 \alpha^1 \mu^0)$	4.665E-11	0.643	3437815.3
I_{18} $(\Delta p^1 n^2 \alpha^2 \mu^0)$	-1.190E-10	0.644	1761356.4

Table 3.8. Continued.

Term	Coeff. value	Coeff. p-value	VIF
I_{19} ($\Delta p^2 n^0 \alpha^0 \mu^0$)	7.369E-15	0.299	71503.5
I_{20} ($\Delta p^2 n^0 \alpha^1 \mu^0$)	-6.450E-14	0.454	521588.6
I_{21} ($\Delta p^2 n^0 \alpha^2 \mu^0$)	1.207E-13	0.576	260227.7
I_{22} ($\Delta p^2 n^1 \alpha^0 \mu^0$)	-8.110E-17	0.333	593755.0
I_{23} ($\Delta p^2 n^1 \alpha^1 \mu^0$)	7.129E-16	0.492	4322610.3
I_{24} ($\Delta p^2 n^1 \alpha^2 \mu^0$)	-1.500E-15	0.568	2179472.0
I_{25} ($\Delta p^2 n^2 \alpha^0 \mu^0$)	2.030E-19	0.304	325158.1
I_{26} ($\Delta p^2 n^2 \alpha^1 \mu^0$)	-1.950E-18	0.429	2404247.4
I_{27} ($\Delta p^2 n^2 \alpha^2 \mu^0$)	4.398E-18	0.481	1220325.4
I_{28} ($\Delta p^0 n^0 \alpha^0 \mu^1$)	4.362E+01	0.548	8172.7
I_{29} ($\Delta p^0 n^0 \alpha^1 \mu^1$)	-3.545E+02	0.705	65914.5
I_{30} ($\Delta p^0 n^0 \alpha^2 \mu^1$)	7.190E+02	0.764	34538.9
I_{31} ($\Delta p^0 n^1 \alpha^0 \mu^1$)	-2.581E-01	0.778	73140.2
I_{32} ($\Delta p^0 n^1 \alpha^1 \mu^1$)	2.928E+00	0.803	582458.4
I_{33} ($\Delta p^0 n^1 \alpha^2 \mu^1$)	-9.818E-01	0.974	303867.4
I_{34} ($\Delta p^0 n^2 \alpha^0 \mu^1$)	3.280E-04	0.883	41989.7
I_{35} ($\Delta p^0 n^2 \alpha^1 \mu^1$)	-2.686E-03	0.925	333609.4
I_{36} ($\Delta p^0 n^2 \alpha^2 \mu^1$)	-8.308E-03	0.909	173583.3
I_{37} ($\Delta p^1 n^0 \alpha^0 \mu^1$)	-2.357E-06	0.826	78295.0
I_{38} ($\Delta p^1 n^0 \alpha^1 \mu^1$)	1.139E-05	0.933	636106.6
I_{39} ($\Delta p^1 n^0 \alpha^2 \mu^1$)	-6.772E-06	0.984	330537.9
I_{40} ($\Delta p^1 n^1 \alpha^0 \mu^1$)	2.681E-09	0.984	690365.3
I_{41} ($\Delta p^1 n^1 \alpha^1 \mu^1$)	6.892E-08	0.967	5541242.2
I_{42} ($\Delta p^1 n^1 \alpha^2 \mu^1$)	-3.987E-07	0.924	2877288.5
I_{43} ($\Delta p^1 n^2 \alpha^0 \mu^1$)	2.792E-11	0.929	387195.5
I_{44} ($\Delta p^1 n^2 \alpha^1 \mu^1$)	-8.140E-10	0.837	3123370.7
I_{45} ($\Delta p^1 n^2 \alpha^2 \mu^1$)	2.456E-09	0.807	1623783.3
I_{46} ($\Delta p^2 n^0 \alpha^0 \mu^1$)	-1.070E-13	0.709	62416.2
I_{47} ($\Delta p^2 n^0 \alpha^1 \mu^1$)	6.141E-13	0.860	479149.0
I_{48} ($\Delta p^2 n^0 \alpha^2 \mu^1$)	-1.050E-12	0.904	242873.1
I_{49} ($\Delta p^2 n^1 \alpha^0 \mu^1$)	8.556E-16	0.801	519946.1
I_{50} ($\Delta p^2 n^1 \alpha^1 \mu^1$)	-8.930E-15	0.830	4036605.9
I_{51} ($\Delta p^2 n^1 \alpha^2 \mu^1$)	1.936E-14	0.853	2067688.7
I_{52} ($\Delta p^2 n^2 \alpha^0 \mu^1$)	-2.800E-18	0.727	284477.8
I_{53} ($\Delta p^2 n^2 \alpha^1 \mu^1$)	3.488E-17	0.725	2249460.2
I_{54} ($\Delta p^2 n^2 \alpha^2 \mu^1$)	-7.940E-17	0.751	1159718.0

The Jeong model explained the flow loss data well at the region of losses, but the error was higher with the larger flow loss data points. Jeong had a similar finding when he first published his model. The model had a RMSE of calibration of 0.896 L/min.

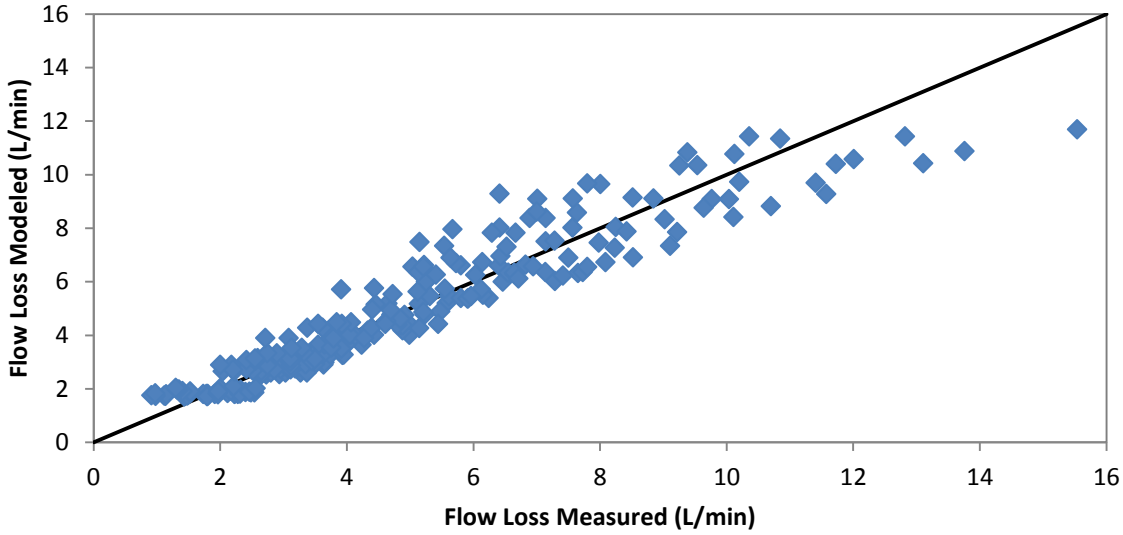

Figure 3.12. Cross plot of measured vs. modeled flow loss, post calibration for the full Jeong flow loss model.

The Jeong flow loss model has a p-value of less than 0.0001 and four of the six variables were statistically different than zero (Table 3.9).

Table 3.9. Model coefficient p-values and variance inflation factor of the full Jeong model.

Model p-value		<.0001*	
Term	**Coeff. value**	**Coeff. p-value**	**VIF**
$C_{\mu PSV}$	4.395E-05	<.0001*	5.0
C_{vPV}	-7.634E-05	0.4039	12.9
C_{VN}	3.780E+00	<.0001*	24.6
C_{PP}	4.361E-14	0.6063	2.0
C_{β}	4.402E-06	<.0001*	10.5
Q_{Lo}	1.482E+00	<.0001*	18.5

However, four of the model coefficients within the model have a VIF greater than 10. This large VIF value leads one to the conclusion that multicollinearity may be an issue and reduction of model terms may improve the model.

The Ivantysyn and Ivantysynova model had the lowest RMSE of calibration (Table 3.10). The Jeong model and the Zarotti and Nevegna flow loss models were next closest at around three times the Ivantysyn and Ivantysynova model. The two physical process-based flow loss models – Wilson and Schlösser – had the largest values of RMSE of calibration.

Table 3.10. RMSE of full model, stepwise regression reduced and multicollinearity reduced models.

Model	Number of Model Terms			Model RMSE (L/min)		
	Full	Stepwise Reduced	Multicollin. Reduced	Full	Stepwise Reduced	Multicollin. Reduced
Wilson	2	2	2	2.446		
Schlösser	2	1	2	2.814	2.828	
Zarotti and Nevegna	5	5	3	1.083		1.400
Ivantysyn and Ivantysynova	54	15	12	0.304	0.305	0.851
Jeong	6	4	6	0.896	0.893	

3.3.2 Stepwise Regression Comparison

After stepwise regression, three of the five models had a reduced number of terms (Table 3.10). In all three, there was only a slight increase in RMSE even though the models had terms reduced. A further discussion of each of the models is below including the model terms that remained after the stepwise regression as well as descriptive statistics about model coefficients that remained. The Wilson and Zarotti and Nevegna models will not be discussed further in this section since they were not different than the full models above.

The Schlösser model was reduced from two terms to one during the stepwise regression. The laminar flow loss term was removed and the RMSE only increased by 0.014 L/min. This result makes sense since in the complete model, the turbulent flow loss term was significant and the laminar was not significant (Table 3.11). However, the Schlösser model had the largest RMSE of calibration in this study.

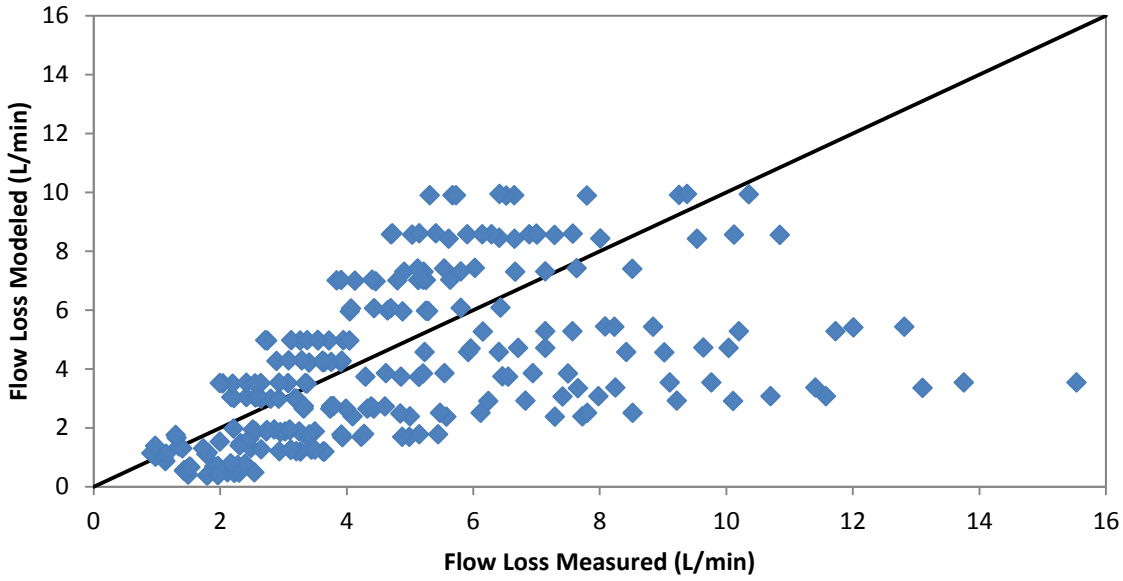

Figure 3.13. Cross plot of measured vs. modeled flow loss, of the post stepwise regression Schlösser flow loss model.

Table 3.11. Model coefficient p-values and variance inflation factor of the post stepwise regression Schlösser model.

Model p-value		<.0001*	
Term	**Coeff. p-value**	**Coeff. p-value**	**VIF**
C_S			
C_{ST}	3.578E+01	<.0001*	1

The number of model terms in the Ivantysyn and Ivantysynova model was reduced from fifty-four to fifteen (Table 3.12). With this reduced flow loss model, the RMSE was only increased by 0.001 L/min, and the measured vs. modeled cross plot

appeared to be nearly indistinguishable from that of the complete model calibration (Fig 3.14). All of the model coefficients were statistically significant, but all of the model terms still have a VIF of greater than 10. This model had the lowest RMSE of the stepwise reduced models, but multicollinearity may still be an issue even with the reduced model as indicated by the VIF values.

Table 3.12. Model coefficient p-values and variance inflation factor of the post stepwise regression Ivantysyn and Ivantysynova model.

Model p-value		<.0001*	
Term	**Coeff. value**	**Coeff. p-value**	**VIF**
I_{01} $(\Delta p^0 n^0 \alpha^0 \mu^0)$	9.633E-01	<.0001*	39.4
I_{02} $(\Delta p^0 n^0 \alpha^1 \mu^0)$			
I_{03} $(\Delta p^0 n^0 \alpha^2 \mu^0)$			
I_{04} $(\Delta p^0 n^1 \alpha^0 \mu^0)$	3.867E-03	<.0001*	40.7
I_{05} $(\Delta p^0 n^1 \alpha^1 \mu^0)$	-1.536E-02	<.0001*	33.2
I_{06} $(\Delta p^0 n^1 \alpha^2 \mu^0)$			
I_{07} $(\Delta p^0 n^2 \alpha^0 \mu^0)$			
I_{08} $(\Delta p^0 n^2 \alpha^1 \mu^0)$			
I_{09} $(\Delta p^0 n^2 \alpha^2 \mu^0)$			
I_{10} $(\Delta p^1 n^0 \alpha^0 \mu^0)$	2.511E-07	<.0001*	90.1
I_{11} $(\Delta p^1 n^0 \alpha^1 \mu^0)$	-3.536E-07	<.0001*	42.9
I_{12} $(\Delta p^1 n^0 \alpha^2 \mu^0)$			
I_{13} $(\Delta p^1 n^1 \alpha^0 \mu^0)$			
I_{14} $(\Delta p^1 n^1 \alpha^1 \mu^0)$			
I_{15} $(\Delta p^1 n^1 \alpha^2 \mu^0)$			
I_{16} $(\Delta p^1 n^2 \alpha^0 \mu^0)$	8.015E-13	<.0001*	83
I_{17} $(\Delta p^1 n^2 \alpha^1 \mu^0)$			
I_{18} $(\Delta p^1 n^2 \alpha^2 \mu^0)$			
I_{19} $(\Delta p^2 n^0 \alpha^0 \mu^0)$			
I_{20} $(\Delta p^2 n^0 \alpha^1 \mu^0)$			
I_{21} $(\Delta p^2 n^0 \alpha^2 \mu^0)$			
I_{22} $(\Delta p^2 n^1 \alpha^0 \mu^0)$	-7.010E-18	<.0001*	176.2
I_{23} $(\Delta p^2 n^1 \alpha^1 \mu^0)$			
I_{24} $(\Delta p^2 n^1 \alpha^2 \mu^0)$			

Table 3.12. Continued.

Term	Coeff. value	Coeff. p-value	VIF
I_{25} $(\Delta p^2 n^2 \alpha^0 \mu^0)$	2.364E-20	<.0001*	180.1
I_{26} $(\Delta p^2 n^2 \alpha^1 \mu^0)$			
I_{27} $(\Delta p^2 n^2 \alpha^2 \mu^0)$			
I_{28} $(\Delta p^0 n^0 \alpha^0 \mu^1)$	2.218E+01	<.0001*	24.3
I_{29} $(\Delta p^0 n^0 \alpha^1 \mu^1)$			
I_{30} $(\Delta p^0 n^0 \alpha^2 \mu^1)$			
I_{31} $(\Delta p^0 n^1 \alpha^0 \mu^1)$			
I_{32} $(\Delta p^0 n^1 \alpha^1 \mu^1)$			
I_{33} $(\Delta p^0 n^1 \alpha^2 \mu^1)$	2.268E+00	<.0001*	45.3
I_{34} $(\Delta p^0 n^2 \alpha^0 \mu^1)$			
I_{35} $(\Delta p^0 n^2 \alpha^1 \mu^1)$	-1.535E-03	<.0001*	37.0
I_{36} $(\Delta p^0 n^2 \alpha^2 \mu^1)$			
I_{37} $(\Delta p^1 n^0 \alpha^0 \mu^1)$	-1.840E-06	<.0001*	91.2
I_{38} $(\Delta p^1 n^0 \alpha^1 \mu^1)$			
I_{39} $(\Delta p^1 n^0 \alpha^2 \mu^1)$	2.385E-05	<.0001*	30.8
I_{40} $(\Delta p^1 n^1 \alpha^0 \mu^1)$			
I_{41} $(\Delta p^1 n^1 \alpha^1 \mu^1)$			
I_{42} $(\Delta p^1 n^1 \alpha^2 \mu^1)$	-6.543E-08	<.0001*	14.6
I_{43} $(\Delta p^1 n^2 \alpha^0 \mu^1)$			
I_{44} $(\Delta p^1 n^2 \alpha^1 \mu^1)$			
I_{45} $(\Delta p^1 n^2 \alpha^2 \mu^1)$			
I_{46} $(\Delta p^2 n^0 \alpha^0 \mu^1)$	-2.790E-14	0.0009*	51.6
I_{47} $(\Delta p^2 n^0 \alpha^1 \mu^1)$			
I_{48} $(\Delta p^2 n^0 \alpha^2 \mu^1)$			
I_{49} $(\Delta p^2 n^1 \alpha^0 \mu^1)$			
I_{50} $(\Delta p^2 n^1 \alpha^1 \mu^1)$			
I_{51} $(\Delta p^2 n^1 \alpha^2 \mu^1)$			
I_{52} $(\Delta p^2 n^2 \alpha^0 \mu^1)$			
I_{53} $(\Delta p^2 n^2 \alpha^1 \mu^1)$			
I_{54} $(\Delta p^2 n^2 \alpha^2 \mu^1)$			

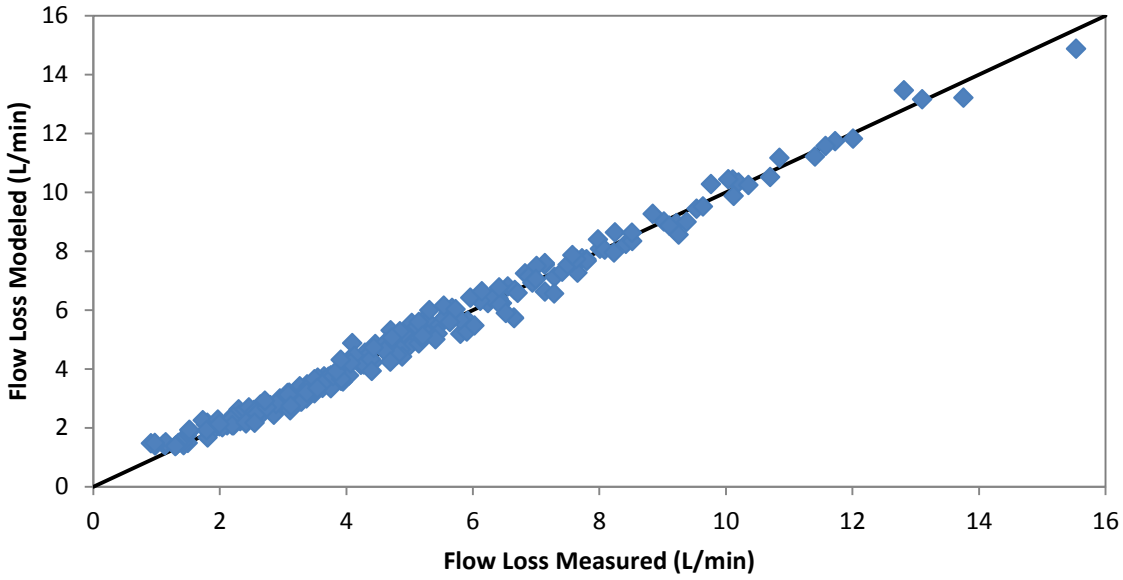

Figure 3.14. Cross plot of measured vs. modeled flow loss, of the Ivantysyn and Ivantysynova flow loss model post stepwise regression.

The Jeong model was reduced to four model terms from the original six (Table 3.13), and the RMSE was reduced by 0.003 L/min (Fig 3.15). All of the remaining model coefficients were significantly different from zero and three of the four had a VIF of less than 10, so only one term, C_{VN}, has any indication of multicollinearity.

Table 3.13. Model coefficient p-values and variance inflation factor of the reduced Jeong flow loss model.

Model p-value		<.0001*	
Term	**Coeff. value**	**Coeff. p-value**	**VIF**
$C_{\mu PSV}$	4.509E-05	<.0001*	4.8
$C_{\nu PV}$			
C_{VN}	3.942E+00	<.0001*	17.8
C_{PP}			
C_{β}	4.171E-06	<.0001*	4.2
Q_{Lo}	1.349E+00	<.0001*	6.4

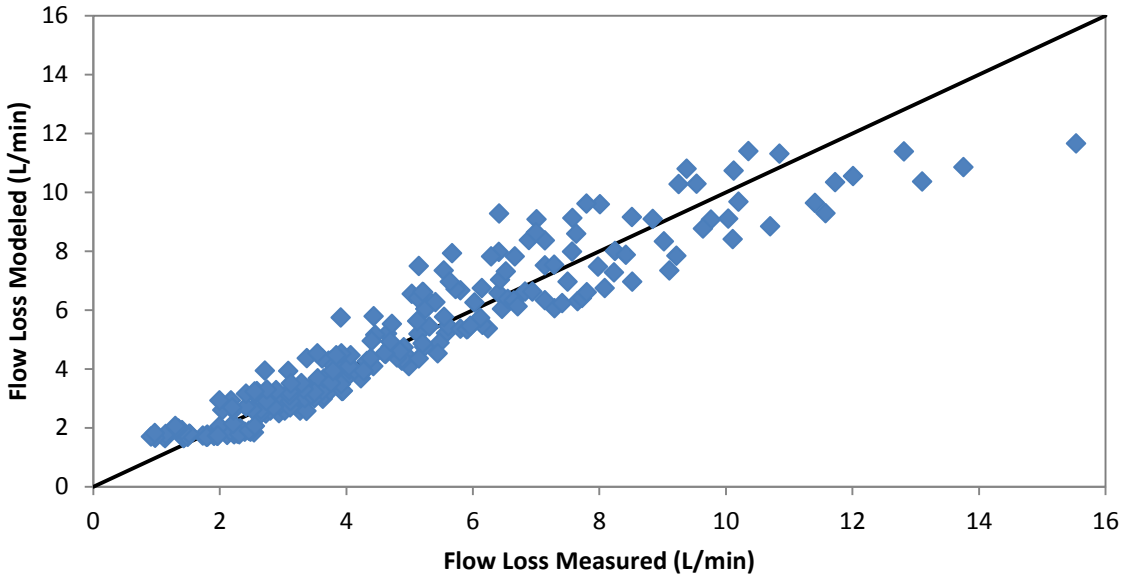

Figure 3.15. Cross plot of measured vs. modeled flow loss, of the Jeong flow loss model post stepwise regression.

3.3.3 Model Reduction by Multicollinearity Analysis

Of the five models, only the Zarotti and Nevegna model and the Ivantysyn and Ivantysynova model had evidence of multicollinearity within them (Correlation Coefficient > 0.85). Only these two models will be discussed in this section.

Examining the correlation matrix for the Zarotti and Nevegna flow loss model in table 3.16, there were two combinations of model terms that were exhibited: 1) C_1 and C_2, and 2) C_3 and C_{45} (Table 3.14).

Table 3.14. Correlation matrix for the Zarotti and Nevegna flow loss model.

	C_1	C_2	C_3	C_{4_5}	C_5
C_1					
C_2	0.9668				
C_3	0.7138	0.7403			
C_{4_5}	0.7618	0.7401	0.9647		
C_5	0.5106	0.4978	0.7968	0.8111	

Of these two relationships, the model coefficients with the larger p value from the complete model calibration were eliminated (C_2 and C_3). As result of this model reduction, only one single coefficient $\boldsymbol{C_{4\_5}}$, had a VIF greater than 10 (Table 3.15).

Table 3.15. Model coefficient p-values and variance inflation factor of the multicollinearity analysis reduced Zarotti and Nevegna model.

Model p-value		<.0001*	
Term	**Coeff. value**	**Coeff. p-value**	**VIF**
C_1	1.353E-07	<.0001*	5.0
C_2			
C_3			
C_{4_5}	6.815E-10	<.0001*	10.6
C_5	-2.720E-12	<.0001*	4.4

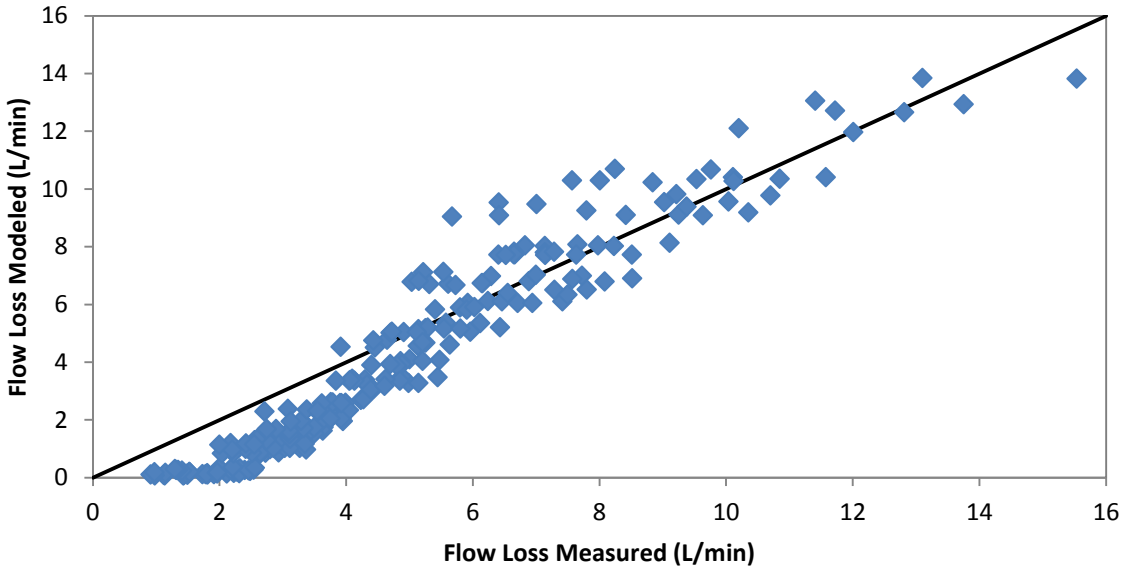

Figure 3.16. Cross plot of measured vs. modeled flow loss, of the reduced Zarotti and Nevegna flow loss model from multicollinearity analysis.

In the case of the Ivantysyn and Ivantysynova model, 122 model term combinations had a correlation coefficient of greater than 0.85 of the 1431 possible combinations of model terms. After going through all 122 model term combinations, and removing the one of the pair that had the larger p-value, twelve of the original

fifty four model terms remained (Table 3.16). However, eight of the twelve model coefficients from the reduced model were significantly different from zero for the reduced model whereas zero of the fifty four model coefficients were non-zero in the complete model. Thus, the amount of multicollinearity has been greatly reduced, but only three of the twelve had a VIF of less than ten. This suggests that the multicollinearity has been greatly reduced, but may still be an issue with the model.

Table 3.16. Model coefficient p-values and variance inflation factor of the post multicollinear reduction Ivantysyn and Ivantysynova model.

Model p-value		<.0001*	
Term	**Coeff. value**	**Coeff. p-value**	**VIF**
I_{01} $(\Delta p^0 n^0 \alpha^0 \mu^0)$	2.289E+00	<.0001*	54.0
I_{02} $(\Delta p^0 n^0 \alpha^1 \mu^0)$			
I_{03} $(\Delta p^0 n^0 \alpha^2 \mu^0)$	-9.393E+00	0.0477*	27.4
I_{04} $(\Delta p^0 n^1 \alpha^0 \mu^0)$	4.448E-03	0.0064*	49.0
I_{05} $(\Delta p^0 n^1 \alpha^1 \mu^0)$			
I_{06} $(\Delta p^0 n^1 \alpha^2 \mu^0)$			
I_{07} $(\Delta p^0 n^2 \alpha^0 \mu^0)$			
I_{08} $(\Delta p^0 n^2 \alpha^1 \mu^0)$			
I_{09} $(\Delta p^0 n^2 \alpha^2 \mu^0)$	-5.482E-05	0.3258	21.3
I_{10} $(\Delta p^1 n^0 \alpha^0 \mu^0)$			
I_{11} $(\Delta p^1 n^0 \alpha^1 \mu^0)$			
I_{12} $(\Delta p^1 n^0 \alpha^2 \mu^0)$			
I_{13} $(\Delta p^1 n^1 \alpha^0 \mu^0)$			
I_{14} $(\Delta p^1 n^1 \alpha^1 \mu^0)$			
I_{15} $(\Delta p^1 n^1 \alpha^2 \mu^0)$			
I_{16} $(\Delta p^1 n^2 \alpha^0 \mu^0)$			
I_{17} $(\Delta p^1 n^2 \alpha^1 \mu^0)$			
I_{18} $(\Delta p^1 n^2 \alpha^2 \mu^0)$			
I_{19} $(\Delta p^2 n^0 \alpha^0 \mu^0)$	4.985E-15	<.0001*	18.7
I_{20} $(\Delta p^2 n^0 \alpha^1 \mu^0)$	-6.660E-15	<.0001*	9.0
I_{21} $(\Delta p^2 n^0 \alpha^2 \mu^0)$			
I_{22} $(\Delta p^2 n^1 \alpha^0 \mu^0)$			
I_{23} $(\Delta p^2 n^1 \alpha^1 \mu^0)$			
I_{24} $(\Delta p^2 n^1 \alpha^2 \mu^0)$			
I_{25} $(\Delta p^2 n^2 \alpha^0 \mu^0)$	2.257E-20	<.0001*	4.3
I_{26} $(\Delta p^2 n^2 \alpha^1 \mu^0)$			

Table 3.16. Continued.

Term	Coeff. value	Coeff. p-Value	VIF
I_{27} $(\Delta p^2 n^2 \alpha^2 \mu^0)$			
I_{28} $(\Delta p^0 n^0 \alpha^0 \mu^1)$	-7.732E+00	0.7135	89.1
I_{29} $(\Delta p^0 n^0 \alpha^1 \mu^1)$	1.823E+02	0.0486*	82.6
I_{30} $(\Delta p^0 n^0 \alpha^2 \mu^1)$			
I_{31} $(\Delta p^0 n^1 \alpha^0 \mu^1)$	1.403E-05	0.9999	85.3
I_{32} $(\Delta p^0 n^1 \alpha^1 \mu^1)$	-3.295E-01	0.3804	77.0
I_{33} $(\Delta p^0 n^1 \alpha^2 \mu^1)$			
I_{34} $(\Delta p^0 n^2 \alpha^0 \mu^1)$			
I_{35} $(\Delta p^0 n^2 \alpha^1 \mu^1)$			
I_{36} $(\Delta p^0 n^2 \alpha^2 \mu^1)$			
I_{37} $(\Delta p^1 n^0 \alpha^0 \mu^1)$			
I_{38} $(\Delta p^1 n^0 \alpha^1 \mu^1)$			
I_{39} $(\Delta p^1 n^0 \alpha^2 \mu^1)$			
I_{40} $(\Delta p^1 n^1 \alpha^0 \mu^1)$			
I_{41} $(\Delta p^1 n^1 \alpha^1 \mu^1)$			
I_{42} $(\Delta p^1 n^1 \alpha^2 \mu^1)$			
I_{43} $(\Delta p^1 n^2 \alpha^0 \mu^1)$			
I_{44} $(\Delta p^1 n^2 \alpha^1 \mu^1)$			
I_{45} $(\Delta p^1 n^2 \alpha^2 \mu^1)$			
I_{46} $(\Delta p^2 n^0 \alpha^0 \mu^1)$	-4.950E-14	<.0001*	8.7
I_{47} $(\Delta p^2 n^0 \alpha^1 \mu^1)$			
I_{48} $(\Delta p^2 n^0 \alpha^2 \mu^1)$			
I_{49} $(\Delta p^2 n^1 \alpha^0 \mu^1)$			
I_{50} $(\Delta p^2 n^1 \alpha^1 \mu^1)$			
I_{51} $(\Delta p^2 n^1 \alpha^2 \mu^1)$			
I_{52} $(\Delta p^2 n^2 \alpha^0 \mu^1)$			
I_{53} $(\Delta p^2 n^2 \alpha^1 \mu^1)$			
I_{54} $(\Delta p^2 n^2 \alpha^2 \mu^1)$			

The model was then calibrated with the measured data set, and the RMSE of the reduced model was 0.851 L/min, which was substantially higher than 0.304 L/min with the complete model (Fig. 3.17). The model overestimates flow loss below 4 L/min, then underestimates the flow loss until 6 L/min. The method reduced the

amount of multicollinearity, but the remaining model terms did not explain flow loss variability as well as the stepwise regression reduced model.

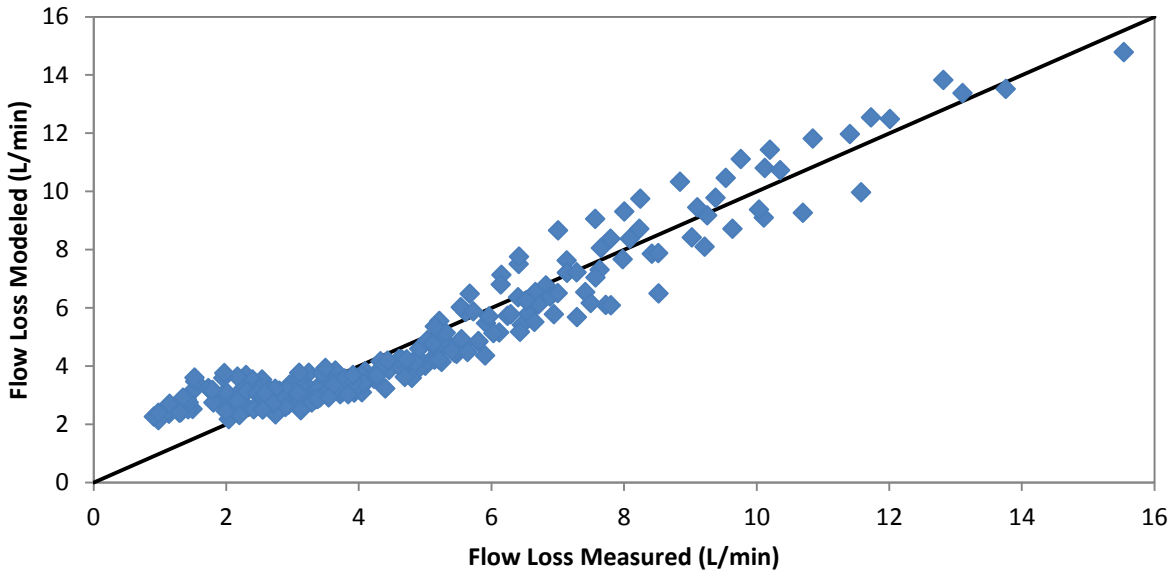

Figure 3.17. Cross plot of measured vs. modeled flow loss, of the reduced Ivantysyn and Ivantysynova flow loss model after multicollinearity analysis.

3.3.4 Leave One Out Cross Validation

The results of the leave one out cross validation are shown in table 3.17. Neither the Wilson nor the Schlösser model had a significant increase in error of cross validation. This result is probably due to their poor calibration performance and to their only having two terms.

The Zarotti and Nevegna model was not reduced by stepwise regression, but the multicollinearity reduction resulted in two model terms being dropped. After performing the LOOCV, it was apparent that the RMSE of cross validation was higher for the multicollinearity reduced model, but the percent increase in RMSE was significantly less than the complete model.

Table 3.17. Validation error and percent increase in RMSE of cross validation compared to RMSE of calibration.

Model	Number of Model Terms			LOOCV RMSE (L/min) (% increase from calibration)		
	Full	Stepwise Reduced	Multicollin. Reduced	Full	Stepwise Reduced	Multicollin. Reduced
Wilson	2	2	2	2.457 (0.4)		
Schlösser	2	1	2	2.823 (0.3)	2.836 (0.3)	
Zarotti and Nevegna	5	5	3	1.094 (4.5)		1.402 (0.1)
Ivantysyn and Ivantysynova	54	15	12	1.105 (263.4)	1.183 (287.9)	2.438 (286.5)
Jeong	6	4	6	0.914 (2.1)	0.912 (1.9)	

The Ivantysyn and Ivantysynova models vary substantially in the number of model terms between the complete model and the two reduced models. The cross validation error increased by more than 260 percent over that associated with calibration for the complete model and by 280 percent for the reduced models. This dramatic increase in RMSE from calibration to cross validation showed that even after the model had been reduced through stepwise regression and multicollinearity analysis, that both reduced models overfit the measured flow loss data set.

The Jeong model was reduced from six to four terms during stepwise regression and there were no collinear pairs in the multicollinearity reduction; this effectively yields only two models for LOOCV. For the two versions of the model,

the cross validation error was approximately two percent greater than that associated with calibration indicating a low degree of overfitting.

From a standpoint of evaluating the predictive capability of the models, the cross validation error associated with the Wilson and Schlösser models indicated that they were not over-fitting, but they never had high performance in explaining flow loss. The remaining three models had similar magnitude cross validation error, except for the reduced Ivantysyn and Ivantysynova model through multicollinearity analysis. Of these three models, the Jeong model had the lowest RMSE of cross validation and showed the best performance in modeling the flow loss for the cross validation data.

3.4 Conclusions

The Ivantysyn and Ivantysynova model clearly had the lowest RMSE when calibrated to the flow loss data set. However, early indications from the VIF and the high model coefficient p-values indicate that overfitting may be an issue. In subsequent sections, the model was shown to have problems with overfitting. The Jeong and Zarotti and Nevegna models were calibrated and produced similar calibration errors at around one liter per minute, and the Wilson and Schlösser models were had error substantly above that.

Stepwise regression only reduced two of the flow loss models: the Ivantysyn and Ivantysynova model and the Jeong Model. The number of model terms in the stepwise reduced Ivantysyn and Ivantysynova model decreased dramatically from fifty four to fifteen. From the subsequent correlation coefficient matrix examination and LOOCV, this dramatic reduction was due to the complete model being too

complex and over fitting the data set. The Jeong model was reduced to four model terms, but it appears that the two model terms were not eliminated due to over fitting, but instead the terms did not add predictive capability to the model.

Through multicollinearity analysis, the Zarotti and Nevegna model and the Ivantysyn and Ivantysynova model were the only models reduced. The Zarotti and Nevegna model had two pairs of collinear model terms. Conversely, the number of model terms in the Ivantysyn and Ivantysynova model decreased dramatically through multicollinearity analysis, but overfitting was still observed in the reduced model.

The Jeong model exhibited the lowest cross validation error providing evidence that it was modeling the flow losses of the pump without fitting to the specific data set. Even though all three versions of the Ivantysyn and Ivantysynova model have a smaller RMSE of calibration, it was evident that the models were overfitting the data set. The Zarotti and Nevegna model also closely models the flow loss phenomena, and with the complete model, has a similar capability to predict flow loss as the Ivantysyn and Ivantysynova model.

In summary, the following conclusions can be drawn from this work

- The Ivantysyn and Ivantysynova had the lowest calibration error, and thus had the highest performance in explaining variability in flow loss. The Jeong model and Zarotti and Nevegna model were nearly equivalent, and had calibration error that was about three times larger than that of the Ivantysyn

and Ivantysynova models. The Wilson and Schlösser models did not show good performance in modeling the flow loss data.

- The Ivantysyn and Ivantysynova model terms were greatly reduced through both reduction methods. However, the stepwise regression reduced model had a much lower RMSE than the multicollinearity analysis reduced model. A reduced Jeong model emerged through step-wise regression analysis, but none results from multicollinearity analysis. The opposite result occurred with the Zarotti and Nevegna model; in neither case did model reduction have a substantial effect on error. The Schlösser model was reduced to only the turbulent term in stepwise regression with minimal change to the error compared to the complete model.
- There appears to be a significant amount of overfitting within the complete and both reduced versions of the Ivantysyn and Ivantysynova model. In all three cases the RMSE of cross validation was nearly three times that of the RMSE of calibration. Given the Jeong model and Zarotti and Nevegna model had a similar RMSE of cross validation compared to the Ivantysyn and Ivantysynova models, **the Jeong model, the Zarotti and Nevegna model and the Ivantysyn and Ivantysynova model estimate the pump flow losses equally well.** The Wilson and Schlösser models do not generalize as well as the other three.

REFERENCES

[1] Federal Register (US), 2004, “Control of Emissions of Air Pollution From Nonroad Diesel Engines and Fuel; Final Rule,” Vol. 69 No. 124, 2004, June 29. Retrieved January 02, 2012, from http://www.gpo.gov/fdsys/pkg/FR-2004-06-29/pdf/04-11293.pdf.

[2] Kenny, K., 2010, “Caterpillar Showcases Tier 4 Interim//Stage IIIB Readiness and Leadership”, press release Feb. 11, 2010, retrieved on 2/8/2014, from http://indonesia.cat.com/cda/files/2076717/7/021110%20Caterpillar%20Showcases%20Tier%204%20Interim%20Stage%20IIIB%20Readiness%20and%20Leadership.pdf.

[3] Love, L., Lanke, E., Alles, P., 2012, “Estimating the Impact (Energy, Emissions and Economics) of the U.S. Fluid Power Industry,” Oak Ridge National Laboratory – United States Department of Energy, ORNL/TM-2011/14.

[4] Wilson, W. 1948. Performance criteria for positive displacement pumps and fluid motors, ASME Semi-annual Meeting, paper No. 48-SA-14.

[5] Ivantysyn J. and Ivantysynova M., 2000, “Hydrostatic Pumps and Motors, Principals, Designs, Performance, Modeling, Analysis, Control and Testing”, New Delhi: Academia Books International.

[6] Schlösser, W., 1961, “Mathematical model for displacement pump and motors,” Hydraulic power transmission, April 1961, pp. 252-257.

[7] Olsson, O., 1973, “Matematisk verkingsgradmodell (Mathematicalv Efficiency Model), Kompendium i Hydraulik” LiTHIKP, Institute of Technology, Linköping, Sweden.

[8] Pacey, D.A., Turnquist, R.O. and Clark, S.J., 1979, “The Development of a Coefficient Model for Hydrostatic Transmissions,” 35th National Conference in Fluid Power, Chicago, IL, USA, pp. 173-178.

[9] Zarotti, L. and Nevegna, N., 1981, “Pump Efficiencies Approximation and Modeling,” 6th International Fluid Power Symposium, Cambridge, UK.

[10] Rydberg, K.-E., 1983, “On performance optimization and digital control of hydrostatic drives for vehicle applications,” Linköping Studies in Science and Technology, Dissertation No. 99, Linköping.

[11] Bavendiek, R., 1987, “Verlustkennwertbestimmung am Beispiel von hydrostatischen Maschinen in Schrägachsenbauweise” Doctoral thesis, VDI Fortschrittsberichte, Reihe 7 Nr. 122, VDI Verlag.

[12] Dorey, R., 1988, “Modelling of losses in pumps and motors,” 1st Bath International Fluid Workshop, University of Bath.

[13] Kögl, C., 1995, “Verstellbare hydrostatische Verdrängereinheiten im Drehzahl- und Drehmomentregelkreis am Netz mit angepasstem Versorgungsdruck,” Doctoral thesis, Institut für fluidtechnische Antriebe und Steuerungen IFAS, RWTH Aachen.

[14] Huhtala, K., 1996, “Modelling of Hydrostatic Transmission – Steady State, Linear and Non-Linear Models,” Mechanical Engineering Series No. 123, Tampere.

[15] Baum, H., 2001, “Einsatzpotentiale neuronaler Netze bei der CAE-Tool unterstützten Projektierung fluidtechnischer Antriebe” Doctoral thesis, Institut für fluidtechnische Antriebe und Steuerungen IFAS, RWTH Aachen.

[16] Ortwig, H., 2002, “New Method of Numerical Calculation of Losses and Efficiencies in Hydrostatic Power Transmissions” SAE International Off-Highway Congress, Las Vegas, NV.

[17] Jeong, H., 2007. “A Novel Performance Model Given by the Physical Dimensions of Hydraulic Axial Piston Motors: Model Derivation”, Journal of Mechanical Science and Technology, Vol 21, No 1, pg. 83-97.

[18] Ott R., Longnecker M., 2001. “An Introduction to Statistical Methods and Data Analysis; Fifth Edition,” pg. 531 – 826.

[19] Gideon E. 1978. "Estimating the dimension of a model,". The annals of Statistics 6, no.2, pg. 461 – 464

[20] International standards organization, “ISO 4409:2007, Hydraulic fluid power -- Positive-displacement pumps, motors and integral transmissions -- Methods of testing and presenting basic steady state performance.”

[21] Toet, G., 1970, “Die Bestimmung des theoretischen Hubvolumensvon hydrostatischen erdrängerpumpen und Motoren aus volumetrischen Messungen,” Ölhydraulik und Pneumatik O+P, 14 (1970) No. 5, pp. 185-190.

[22] Kahane L.H., 2008, “Regression Basics, Second edition” Sage Publications, Inc. : 119-122.

[23] Haan, C. T., 2002, “Statistical methods in Hydrology, Second Edition,” Wiley.

[24] Kutner M.H., Nachtsheim C.J., Neter J., 2004, “Applied Linear Regression Models, 4th edition,” McGraw-Hill Irwin.

[25] Geisser, S., 1993, “Predictive Inference,” Chapman and Hall.

DEFINITIONS, ACRONYMS, ABBREVIATIONS

EPA: Environmental Protection Agency
NOx: Nitrous Oxide
OLS: Ordinary Lest Squares
RMSE: Root Mean Squared Error
BIC: Bayesian Information Criterion

Flow Loss Modeling

C_1, C_2, C_3, C_4, C_5	Loss coefficients (Zarotti and Nevegna model)
$C_{constant}$	Constant flow loss coefficient
C_S	Laminar flow loss coefficient
C_{ST}	Turbulent flow loss coefficient
C_{vPV}	Couette flow coefficient of the Jeong flow loss model
C_{VN}	Valve plate notch loss coefficient (Jeong model)
$C_{\mu PSV}$	Laminar flow loss coefficient (Jeong model)
C_{β}:	Bulk modulus loss coefficient (Jeong model)
$I_{01} - I_{54}$	Model coefficients with exponents 2,2,2 and 1 (Ivantysyn and Ivantysynova model)
k	Kinematic viscosity constant
k_{ijkl}	Loss coefficient (Ivantysyn and Ivantysynova model)
n_{pump}	Pump input shaft speed
Δp_{sys}	Pressure rise from the pump inlet to outlet
$Q_{B.mod}$	Effective flow due to fluid decompression
Q_{ideal}	Flow from pump based on ideal displacement
Q_L	Total flow loss
$Q_{L,ext}$	Flow losses that flow into the pump case

$Q_{L,int}$	Flow losses that flow back to the pump inlet
Q_{Lo}	Constant flow loss (Jeong model)
Q_{meas}	System flow measured after the relief valve
Q_{outlet}	System flow out of the pump
T_{oil}	Oil temperature relative to a reference condition
V_p	Ideal pump displacement
β_0	Reference bulk modulus of the fluid.
β_p	Isothermal compressibility coefficient of fluid,
β_T	Volumetric expansion coefficient of fluid,
η_0	Reference kinematic viscosity
μ	Hydraulic fluid viscosity
ρ	Hydraulic fluid density
ρ_0	The oil density at a reference condition
ρ_T	Rate of change of oil density with temperature

Regression, Multicollinearity and Cross Validation

k:	Number of independent coefficients in a linear model
$\hat{L}$:	Maximized value of the likelihood function for a model
n:	Number of samples in the regression data set
R	Pearson correlation coefficient
R^2	Coefficient of determination of a model coefficient
X	Independent variable (linear regression)
y	Dependent variable (linear regression)
$\hat{y}$	Modeled value of the independent variable
β	Regression coefficient (linear regression)
$\hat{\beta}$	Estimated regression coefficient (linear regression)
ε	Error (linear regression)

CHAPTER 4. GENERAL CONCLUSIONS

4.1 Conclusions

The overall objective of this work was to present a methodology for comparing flow loss models for axial piston pumps. After reviewing the literature, it is apparent that the authors of the flow loss models took great care in developing models based on knowledge of pumps and were able to calibrate the model coefficients with measured data sets. However, statistical issues may arise when building models constructed of model terms representing the flow loss behavior associated with different pump locations, but are nearly linearly related in their loss behavior.

This methodology first considered calibration of each of the models using ordinary least squares linear regression. Nearly all of the models were reducible by one of the two methods and yielded a reduced model that had a similar error of calibration as the full models. The Ivantysyn and Ivantysynova model had the lowest error of calibration.

The full and reduced models were cross validated. In the end, the leave one out cross validation demonstrated that even if the Ivantysyn and Ivantysynova model was reduced, it still overfits the data. To that end, the Jeong model and Zarotti and Nevegna models were just capable of generalizing the data as the Ivantysyn and Ivantysynova model. Ultimately, the objective of any type of statistical model is to represent the physical phenomena as closely as possible, while not overfitting the particular data set used for model calibration.

4.2 Recommendations for Future Work

There are several areas where this work could be expanded to gain a deeper understanding of losses within axial piston pumps. Some potential areas are described as:

- In this work, only flow losses were considered. In nearly all of the models reviewed in chapter 2, each author had a torque loss model as well. A similar study could investigate torque loss models. In general, the number of terms in torque loss models is larger, and it would be of interest to see if the data would support torque model reduction with fewer torque loss terms.
- This study used linear regression to determine the values of the model parameters. Using this analysis, it is possible that some flow loss model terms are negative, but a negative flow loss does not intuitively make sense. A study of alternate statistical methods for determining model parameters could be carried out. Especially in component interaction physical loss models, model parameters could be constrained to correlate to physical dimensions in the pump. Non-linear optimization methods are capable of determining model parameters that can only vary within a user-defined range.
- This research was carried out on one data set from one pump. Given that axial piston pumps do have manufacturing variation within a population, the amount of flow loss in any given pump model is likely to also vary. This variation should be studied, and if specific flow loss parameters are significant across a large number of pumps, this knowledge will aid in ensuring that the

losses are similar to the source of loss that is expected for a particular pump design.

- This study only considered a single design and displacement of axial piston pump. If there is a distinct difference in the design of a set of pumps, it would be of great interest to see if these design differences can be correlated to the terms that are dominant in the flow loss model. Also, comparisons of pumps within a family but different displacements could also be of interest to the pump designer.

ACKNOWLEDGEMENTS

I would first like to give thanks to the creator, and my personal lord and savior, Jesus Christ. I will always appreciate the opportunity that I have been given by him for my time at Iowa State. “Every good gift and every perfect gift is from above, coming down from the Father of lights with whom there is no variation or shadow due to change” [James 1:17, ESV].

I would like to express my thanks and love to my lovely wife Shelly for her near infinite patience with me during my graduate studies. I would like to acknowledge that she did work harder than I did for this degree even though she did not make the first key stroke or solve the first differential equation. I would also like to thank Elaine Christine Hall, Kyler Orlen Hall, Caroline Anne Hall and Meredith Ellyn Hall for being patient as “Daddy finished grad school”.

I would like to express my thanks to my Major Professor Brian Steward. I have appreciated his insight and experience in aiding me with my graduate studies. I believe that his guidance to constantly seeking the reasoning in problem and being able to “tell the story” of a novel solution have been invaluable to this point and tenfold more for the rest of my career. I look to him as an example in how to live as a good christian and a good engineer in all situations.

I would like to thank everyone in the Power Solutions division of Danfoss Corporation. In particular I would like to thank Michael Betz for inspiring me to work towards a Master’s of Science, Jay Moline for believing in me enough to bring me back to Danfoss after the 2009 downturn, Charles Throckmorton for inspiration and assistance in technical writing and his vast Engineering knowledge. I would also like

to thank my team leader James Eisenmenger for his support of my thesis work. I would also like to thank the H1 product development team in Ames for providing the flow loss data set that was used in Chapter 3.

BIOGRAPHICAL SKETCH

Samuel Jason Hall was born on February 23, 1980 in Indianapolis, Indiana. He received the Bachelor of Science in Agricultural and Biological Engineering from Purdue University, West Lafayette in December 2002. He has previously been employed as a Process/ Tool Design Engineer for NetShape Technologies. Sam is currently a Systems and Applications Engineer in the Power Solutions Division of Danfoss and has been with the company in various Engineering roles for nearly seven years.

Sam is the proud husband of Shelly Jean Hall and the father of four children: Elaine Christine Hall, Kyler Orlen Hall, Caroline Anne Hall, and Meredith Ellyn Hall.